

FOR REFERENCE

NOT TO BE TAKEN FROM THIS ROOM

NUMERICAL ANALYSIS
OF
SEMICONDUCTOR DEVICES

by

TUĞRUL TEKBULUT

Submitted to the School of Engineering
in partial fulfillment for the requirements of
Master of Science in
Electrical Engineering

Bogazici University Library



39001100316077

14

Bogaziçi University

Bebek-Istanbul

May-1983

ACKNOWLEDGEMENTS

I would like to acknowledge gratefully my debt to Prof.Dr. Sabih Tansal,my thesis supervisor,whose help,guidance and encouragement made this work possible.

I am indebted to several other persons; a few of whom I can state are my brother Haluk Tekbulut who helped me in writing, running and debugging many of my programs,Zafer Erbaş of Computer Center,and, my friend Ersin Karabudak who wrote the assembly routines of MINIMOS.

ÖZETÇE

Tümleşik devre teknolojisindeki gelişmeler, özellikle çok büyük çapta tümleşim, deneysel araştırmaların zaman harcıyıcı ve pahalı olması nedeniyle bilgisayar destekli tasarımı çok önemli bir gereklilik olarak ortaya çıkarmıştır.

Bu tezde yarı iletken devre elemanlarının nümerik analizine bir giriş yapılmaktadır. Yarı iletken fiziğinin özlü bir tekrarıyla temel yarı iletken denklemleri çıkarılmıştır. Bu denklemlerin çözümü için bir algoritma sunulmuş ve bir boyutlu uzayda uygulaması geniş bir şekilde incelenmiştir. İki ve üç boyutlu uzayda çözümün ortaya koyduğu sorunlar tartışılmış, çeşitli algoritmalar karşılaştırılmıştır. Ayrıca çok geniş matris dizgelerinin çözümünün matematiksel temelleri verilmiştir. Son olarak bir boyutlu analizin sonuçları sunulmuş ve tartışılmıştır.

ABSTRACT

Very large scale integration made computer aided design an urgent necessity in modern design process, since experimental investigations are very time consuming, often too expensive, and sometimes not feasible.

In this thesis, we make an introduction to the numerical analysis of semiconductor devices. The fundamental semiconductor equations are derived with brief review of semiconductor physics. An algorithm for the numerical solution of these equations is described, and its implementation in one dimension is thoroughly explained. The problems of higher dimensional simulation are discussed; various algorithms are compared. Some mathematical background is established for the solution of large matrix systems. And the results of one dimensional simulation are presented and discussed.

TABLE OF CONTENTS

ACKNOWLEDGEMENTS

ÖZETÇE

ABSTRACT

| | |
|---|----|
| I- INTRODUCTION | 1 |
| II- CHARGE TRANSPORT IN SEMICONDUCTORS | 3 |
| III- INTRODUCTION TO THE NUMERICAL SOLUTION OF SEMICONDUCTOR EQUATIONS | 13 |
| IV- TWO DIMENSIONAL NUMERICAL ANALYSIS- AN OVERVIEW | 29 |
| - Solution of Matrix Equations by iterative methods | 35 |
| V- MINIMOS PROGRAM- A TWO DIMENSIONAL MOS TRANSISTOR ANALYZER | 44 |
| VI- DISCUSSION OF RESULTS AND CONCLUSION | 50 |
| APPENDIX A Mathematics of 1-D diode and transistor analysis | 59 |
| APPENDIX B Calculation of guess solutions for DIODE and PNP programs | 65 |
| REFERENCES | 69 |

CHAPTER I

INTRODUCTION

All major advances in the history of economic endeavor are the results of new or improved production methods which make it possible to produce more goods for less human effort. In our age of fast technological growth, one major bottleneck impeding this progress is the scarcity of available engineering time and skilled labor which become inefficient to respond the increasing demand on better and more products. The solution seems to be found in the application of computers both in design and manufacturing.

The electronics industry is now at the point of designing and producing complex systems integrated on a silicon chip. The designer who claims this challenge of putting more on smaller real-estate relies heavily on digital computers in designing devices, process and circuit lay-out.

In this thesis, we shall deal with computer aided device design and analysis from the point of view of numerical analysis

In order to accurately analyse a semiconductor structure the partial differential equations which govern its physical behavior must be solved. In Chapter II, we make a brief introduction to semiconductor physics and derive these equations.

In Chapter III, one dimensional diode and transistor analysis is considered. In Chapter IV, analysis of Chapter III is extended to two dimensions. Various solution techniques are compared, iterative solution of matrix equations are explained. With all of these, MINIMOS program is examined, and the problems of MOS transistor simulation is discussed.

In Chapter VI, we present and discuss the results of DIODE and PNP programs developed on the method explained in Chapter III. Recommendations are given to improve the programs to cover more physical cases.

CHAPTER II

CHARGE TRANSPORT IN SEMICONDUCTORS

Current flow in semiconductors occur in two ways:[3]

(a) when an electric field is applied; (b) when a gradient in the carrier concentration is maintained. The first causes a current flow due to carrier drift; the second gives current flow due to diffusion.

Carrier drift:

The charge flow due to drift of holes is expressed as:

$$\bar{J}_p = q\mu_p p \bar{E} = \sigma_p \bar{E} \quad (2.1.a)$$

where q is the electronic charge, μ_p mobility and p is the volume density of holes. Similar expression holds for electrons:

$$\bar{J}_n = q\mu_n n \bar{E} = \sigma_n \bar{E} \quad (2.1.b)$$

As can be seen current is proportional to the electric field and Ohm's law is valid.

Carrier diffusion:

If there is a concentration gradient of holes, there will be a net charge flow from high to low concentration areas. So, the charge flow must be proportional to $-\nabla p$. The diffusion current of holes with charge q can be expressed as:

$$\bar{J}_p = -qD_p \nabla p \quad (2.2.a)$$

Similarly for electrons:

$$\bar{J}_n = qD_n \nabla n \quad (2.2.b)$$

where D_p and D_n are the hole and electron diffusion constants, respectively. If both drift and diffusion exist, equations (2.1) and (2.2) must be combined.

$$\bar{J}_p = q\mu_p p \bar{E} - qD_p \nabla p \quad (2.3)$$

$$\bar{J}_n = q\mu_n n \bar{E} + qD_n \nabla n \quad (2.4)$$

By introducing the quasi-Fermi level for holes and electrons equations (2.3), (2.4) can be written as an extended version of Ohm's law. If we denote the hole quasi-Fermi potential by φ_p and electron quasi-Fermi potential by φ_n :

$$p = n_i e^{-q(\psi - \varphi_p)/kT} \quad n = n_i e^{q(\psi - \varphi_n)/kT} \quad (2.5)$$

where ψ is the electrostatic potential.

Using the relation $\nabla\psi = -\bar{E}$

and Einstein's relation $\frac{D_p}{\mu_p} = \frac{D_n}{\mu_n} = \frac{kT}{q}$

we obtain: $\bar{J}_p = -q\mu_p p \nabla\varphi_p \quad (2.6)$

$$\bar{J}_n = -q\mu_n n \nabla\varphi_n \quad (2.7)$$

Recombination of carriers:

Many semiconductor devices are based upon the principle of injection of holes into n-type material or injection of electrons into p-type material. Such injected carriers are called minority carriers to distinguish from the majority carriers. These minority carriers will sooner or later recombine with the majority carriers and thus be permanently removed. In principle such a recombination might take place in a single step according to the process:

free electron + free hole \rightleftharpoons electron bound in the valence band
but in many cases, such a recombination occurs in a two-step process involving recombination centers.

A recombination center is a center that can act as an electron trap when empty, and a hole trap when filled. Let holes be injected into n-type material, and let a particular center be

occupied by an electron. It may then act as a hole trap; in the trapping process the electron combines with a free hole, with release of excess energy, thus leaving the center empty. The center can now act as an electron trap; in the trapping process an electron from the conduction band makes a transition to the empty center, with release of excess energy. One hole-electron pair is this way taken out of circulation after completion of such a two-step process.

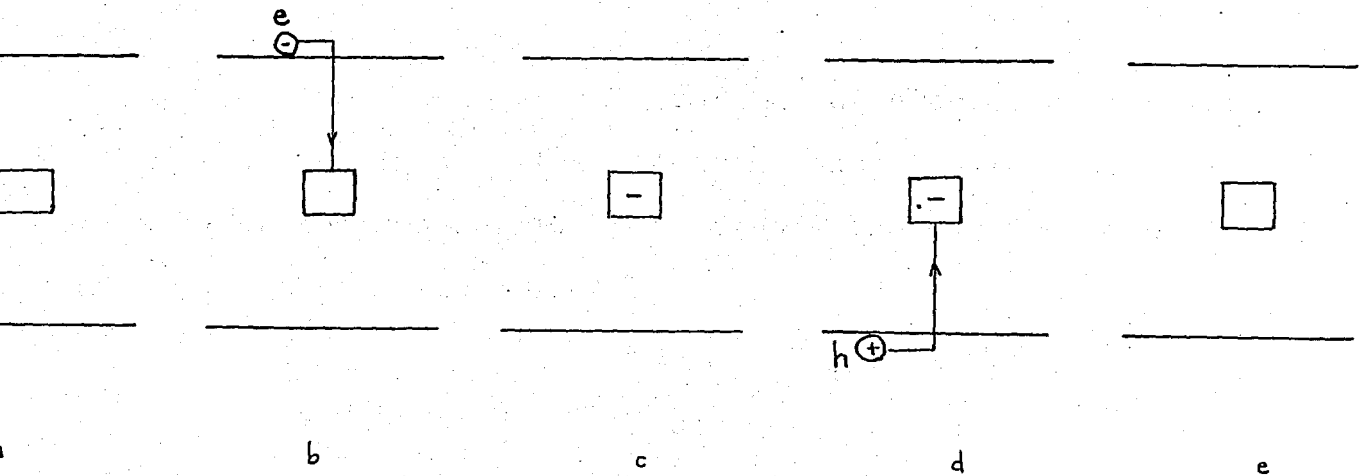


Fig.2.1 Operation of a recombination center. (a) Empty level (b) Electron captured by center (c) Center now negatively charged (d) Hole captured by center (e) Original center restored.

Shockley-Read Theory of Recombination:

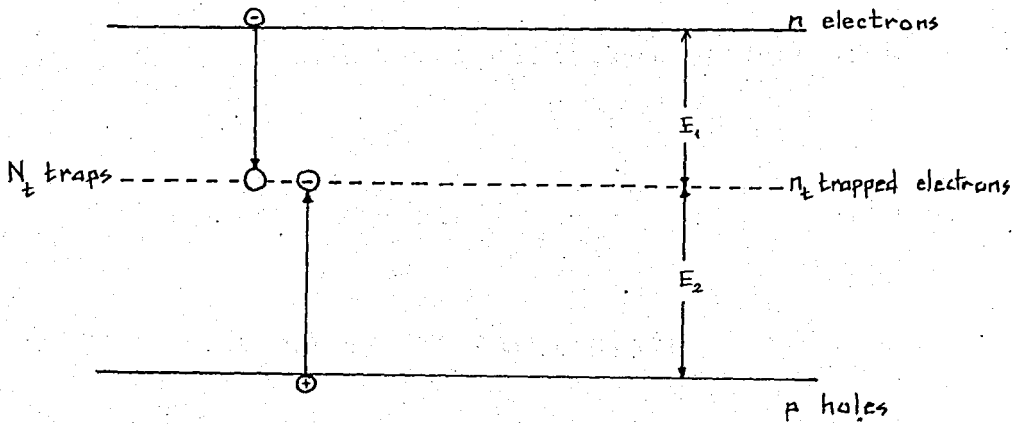


Fig.2.2

Let us first consider the trapping of electrons from the conduction band. If n is the electron concentration and f_t the fraction of traps occupied by electrons, the capture rate R_c may be written in the form

$$R_c = C_n n (1 - f_t) \quad (2.8)$$

where C_n gives the capture rate per electron if all traps are empty. The rate of emission R_e from the traps will be proportional to f_t and hence

$$R_e = C'_n f_t \quad (2.9)$$

In equilibrium $R_c = R_e$ or $C_n' = \frac{C_n n_o (1-f_{to})}{f_{to}}$ (2.10)

where n_o and f_{to} are the equilibrium values of n and f_t . Since

$$\frac{1-f_{to}}{f_{to}} = \exp\left(\frac{E_t - E_f}{kT}\right) \quad (2.11)$$

where E_t is the energy of the trapping level. Also, if the system is nondegenerate

$$n_o = N_c \exp\left(\frac{E_f}{kT}\right) \quad N_c = 2\left(\frac{2\pi m_n^* kT}{h^2}\right)^{3/2} \quad (2.12)$$

Consequently

$$C_n' = C_n N_c \exp\left(\frac{E_t}{kT}\right) = n_1 C_n \quad (2.13)$$

where n_1 is the density of electrons in the conduction band when the Fermi level coincides with the trapping level. The net rate of trapping may thus be written as

$$R_n = C_n (1-f_t)n - C_n n_1 f_t \quad (2.14)$$

In exactly the same way the net rate of trapping for holes is

$$R_p = C_p f_{tp} - C_p p_1 (1-f_t) \quad (2.15)$$

where p_1 is the density of holes in the valence band when the Fermi level coincides with the trapping level.

If we now have a disturbing influence that creates hole-electron pairs at the constant rate R , and steady state conditions have been established, then

$$R = R_n = R_p \quad (2.16)$$

Substituting (2.14) and (2.15) solving for f_t

$$f_t = \frac{nC_n + p_1 C_p}{C_n(n+n_1) + C_p(p+p_1)} \quad (2.17)$$

Substituting (2.17) back into (2.1) the recombination rate R may be written as

$$R = \frac{pn - n_i^2}{(n+n_1)\tau_p + (p+p_1)\tau_n} \quad \tau_p = \frac{1}{C_p} \quad \tau_n = \frac{1}{C_n} \quad (2.18)$$

where τ_p and τ_n are the hole and electron lifetimes respectively.

Continuity equations:

If in a semiconductor sample there is an excess concentration of minority carriers, then the excess carrier concentration can disappear in two ways: by recombination with the majority

carriers and by minority carrier flow.

Consider holes in n-type semiconductor. If R is the recombination rate and G is the generation rate of hole-electron pairs then:

$$\frac{\partial p}{\partial t} = -R + G \quad (2.19)$$

If there is a net flow of holes, then a term must be added to equation (2.19). Consider current flow in the x-direction. If $J_{px}(x)$ is the x component of the hole current density at x , then the x component of that current at $x + \Delta x$ is,

$$J_{px}(x + \Delta x) = J_{px}(x) + \frac{\partial J_{px}}{\partial x} \Delta x$$

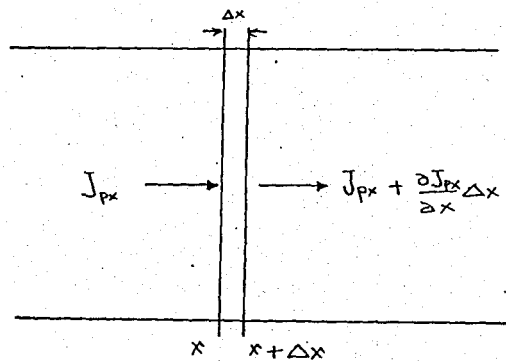


Fig. 2.3

The net number of holes arriving per second in a volume element of unit cross section and width Δx is:

$$- \frac{\partial J_{px}}{\partial x} \cdot \Delta x$$

Dividing by x , we write the net rate of increase in the hole density due to current flow in the x -direction as:

$$- \frac{1}{q} \frac{\partial J_{px}}{\partial x}$$

Adding this to equation (2.19) we get the net rate of change of hole concentration.

$$\frac{\partial p}{\partial t} = -R + G - \frac{1}{q} \frac{\partial J_{px}}{\partial x} \quad (2.20)$$

In three dimensions (2.20) is written in vectoral notation:

$$\frac{\partial p}{\partial t} = -R + G - \frac{1}{q} \nabla \cdot \bar{J}_p \quad (2.21)$$

and for electrons,

$$\frac{\partial n}{\partial t} = -R + G + \frac{1}{q} \nabla \cdot \bar{J}_n \quad (2.22)$$

Equations (2.21) and (2.22) are called continuity equations.

Space charge in semiconductors:

According to Gauss's law, a space charge distribution $\rho(x,y,z)$ is accompanied by an electric field \bar{E} such that

$$\nabla \cdot \bar{E} = \frac{\rho}{\epsilon \epsilon_0} \quad (2.23)$$

where ϵ is the relative permittivity of the medium and ϵ_0 is the permittivity of the free space. Since $\bar{E} = -\nabla\psi$ (2.23) may be written

$$\nabla^2 \psi = -\frac{\rho}{\epsilon \epsilon_0} \quad (2.24)$$

In a semiconductor in equilibrium a net space charge may be present. But according to Gauss's law, this space charge is accompanied by an electric field E . Because of this field there will be a drift term in the electric current. But since there can be no net current flow in equilibrium, the drift term in the current must be exactly balanced by a diffusion current. Only in nonequilibrium cases can a net current flow.

Space charge is generally present in n-type and p-type semiconductors with a nonuniform donor or acceptor concentration. For a semiconductor doped both with donors and acceptors Poisson's equation is of the form:

$$\nabla^2 \psi = -\frac{q}{\epsilon \epsilon_0} (p - n + N_D^+ - N_A^-) \quad (2.25)$$

N_D^+ : concentration of donors,

N_A^- : concentration of acceptors, assuming complete ionization of dopants.

CHAPTER III

INTRODUCTION TO NUMERICAL SOLUTION OF SEMICONDUCTOR EQUATIONS

The first paper on the numerical analysis of semiconductor devices which appeared in 1964 was Gummel's "A self consistent iterative scheme for one dimensional steady state transistor calculations". The approach that he presented in his paper is now called Gummel's algorithm, and it is one of the two basic approaches taken in the numerical analysis of semiconductor devices. In this chapter, we will present a solution method based on Gummel's idea of solving the charge transport equations serially (decoupling), and derive the relevant equations for analysis.

Gummel's Algorithm:

The classical theory of transistors developed by Shockley is based on dividing the transistor into field-free regions where the carriers move only by diffusion, and to space charge regions where there are only ionized impurities and no free carriers.

Shockley theory is successful in describing the behavior

of abrupt junction transistors under low injection conditions. If a transistor's basewidth becomes comparable to the space charge regions, or it has a graded base, the analysis fails. Then numerical methods must be employed.

In the previous chapter, we have shown that the state of a region of a semiconductor material is specified, if the hole and electron concentrations and the electric field are known. Equivalent information is provided by the electrostatic potential ψ and the hole and electron quasi-Fermi potentials. (ϕ_p, ϕ_n) These quantities are governed by a set of three second order nonlinear equations. The basic Gummel Algorithm [1] solves them in the following way:

- 1) A guess solution for the electrostatic potential is entered.

- 2) Hole quasi-Fermi potential and electron quasi-Fermi potentials are calculated through integration. With the guess solution for electrostatic potential this yields hole and electron concentrations.

- 3) Poisson's equation is solved to obtain a better approximation for the electrostatic potential.

- 4) Steps (2) and (3) are alternately executed until the solution is obtained to the required accuracy. (Fig. 3.1)

Input data for calculations are:

- 1) Doping profile,

2) Mobility as a function of doping profile and electric field.

3) Excess carrier recombination model; for Shockley-Read model, the hole and electron lifetimes and the energy of the center are specified.

4) Applied voltages,

5) A trial solution for the electrostatic potential. Boltzmann statistics are used throughout. This limits our application to nondegenerate semiconductors.

Derivation of the one-dimensional solution method:

Variables are normalized as shown in the table below.

| Normalizing constant | Normalized variables |
|---|------------------------|
| $\frac{kT}{q} = V_T$ | ψ, ψ_p, ψ_n |
| n_i | p, n, N_D^+, N_A^- |
| μ_0 | μ_p, μ_n |
| D_0 | D_p, D_n |
| $\left(\frac{kT\epsilon\epsilon_0}{q^2 n_i}\right)^{1/2} = L_D$ | x |
| $\frac{q D_0 n_i}{L_0}$ | J_p, J_n |
| $\frac{D_0 n_i}{L_D^2}$ | R |

Table 3.1

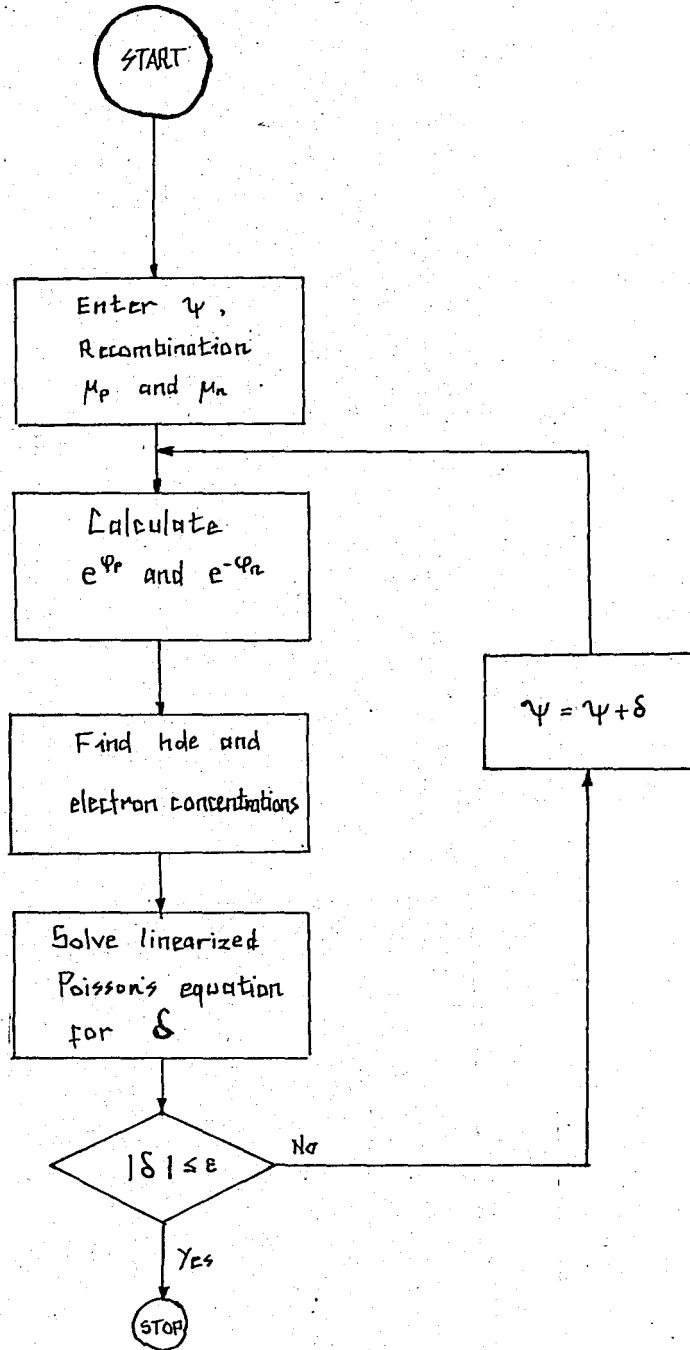


Fig. 3.1

In normalized notation,

hole density: $p = \exp(\varphi_p - \psi)$ (3.1a)

electron density: $n = \exp(\psi - \varphi_n)$ (3.1b)

$$J_p = - \frac{D_p}{D_o} \exp(-\psi) \frac{d}{dx} \exp(\varphi_p) \quad (3.2)$$

$$J_n = - \frac{D_n}{D_o} \exp(-\psi) \frac{d}{dx} \exp(-\varphi_n) \quad (3.3)$$

If no recombination takes place the current densities J_p and J_n are constant.

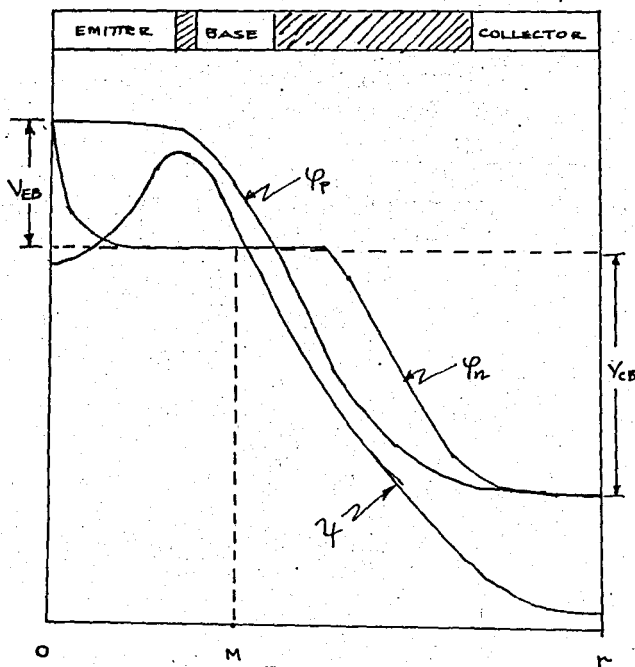


Fig. 2.2

The electrostatic potential is governed by the Poisson's equation

$$\frac{d^2 \psi}{dx^2} = \exp(\psi - \varphi_n) - \exp(\varphi_p - \psi) - N_D^+ - N_A^- \quad (3.4)$$

Imposition of boundary conditions : (Fig.3.2)

- 1) At the end points carrier equilibrium exists ($\varphi_p = \varphi_n$)
This means no excess carriers at the end points.
- 2) Space charge neutrality exists at the metal contacts

$$\frac{d^2 \psi(0)}{dx^2} = \frac{d^2 \psi(r)}{dx^2} = 0.$$

which fixes ψ if $\varphi_p = \varphi_n$ is known.

$$\psi(0) = \varphi_p(0) - \ln\left(\sqrt{\left(\frac{N(0)}{2}\right)^2 + 1} - \frac{N(0)}{2}\right) \quad (3.5)$$

$$\psi(r) = \varphi_p(r) - \ln\left(\sqrt{\left(\frac{N(r)}{2}\right)^2 + 1} - \frac{N(r)}{2}\right) \quad (3.6)$$

$$3) \quad \varphi_p(0) = \varphi_n(0) = \frac{qV}{kT}$$

and

$$\varphi_p(0) = \varphi_n(0) = \frac{qV_{eb}}{kT}$$

$$\varphi_p(r) = \varphi_n(r) = q \frac{V_{cb}}{kT}$$

$$\varphi_n(M) = 0.$$

For transistors we take the reference level for potentials the value of the electron quasi-Fermi level at some point in the base, and set $\varphi_n(M) = 0$. (x) For diodes the reference point is the cathode contact. Usually the choice of the point M is not critical since the electron quasi-Fermi potential has a nearly constant value throughout the base. If φ_n changes considerably across the base, the details of how the base current is brought into the base becomes important and a one dimensional calculation is inadequate.

Now let us compute the hole quasi-Fermi potential and the electron quasi-Fermi potential in terms of the electrostatic potential ψ and the relative diffusion coefficients:

$$\gamma_p = \frac{D_o}{D_p} \quad \gamma_n = \frac{D_o}{D_n} \quad (3.7)$$

From (3.2)

$$\frac{d}{dx} \exp(\varphi_p) = -J_p \gamma_p \exp(\psi) \quad (3.8)$$

Integrating both sides,

$$\exp(\varphi_p(x)) = - \int_0^x J_p(t) \cdot \gamma(t) \cdot \exp(\psi(t)) dt + C \quad (3.9)$$

(x) Here we analyze pnp transistors.

Evaluation of constant C is easy. ($J_p = \text{constant}$, no recombination)

$$\exp(\varphi_p(o)) = - \int_0^o J_p \gamma(t) \exp(\psi(t)) dt + C$$

$$C = \exp(\varphi_p(o))$$

$$\exp(\varphi_p(r)) = - \int_0^r J_p \gamma(t) \exp(\psi(t)) dt + \exp(\varphi_p(o))$$

then
$$J_p = \frac{\exp(\varphi_p(o)) - \exp(\varphi_p(r))}{F(o)} \quad (3.10)$$

where
$$F(o) \triangleq \int_0^r \gamma_p(t) \exp(\psi(t)) dt \quad (3.11)$$

then
$$\exp(\varphi_p(x)) = \frac{\exp(\varphi_p(r)) - \exp(\varphi_p(o))}{F(o)} \int_0^x \gamma_p(t) \exp(\psi(t)) dt + \exp(\varphi_p(o)) \quad (3.12)$$

Proceeding in the same way, we obtain the electron quasi-Fermi potential function as:

$$\exp(-\varphi_n(x)) = \frac{\exp(-\varphi_n(r)) - \exp(-\varphi_n(o))}{F_n(o)} \int_0^x \gamma_n(t) \exp(-\psi(t)) dt + \exp(-\varphi_n(o)) \quad (3.13)$$

where
$$F_n(0) \triangleq \int_0^r \gamma_n \exp(-\psi(t)) dt \quad (3.14)$$

The above equation is valid for diodes, but in the transistor problem the electron quasi-Fermi potential must be specified in two regions. They can be easily derived as

$$\exp(-\varphi_n(x)) = \frac{1 - \exp(-\varphi_n(0)) \int_0^x \gamma_n(t) \exp(-\psi(t)) dt + \exp(-\varphi_n(0)) \int_0^M \gamma_n(t) \exp(-\psi(t)) dt}{\int_0^M \gamma_n(t) \exp(-\psi(t)) dt}$$

where $0 \leq x < M$ (3.15)

$\varphi_n(M) = 0$. M is a point in the base, choice of which is not very important.

$$\exp(-\varphi_n(x)) = \frac{\exp(-\varphi_n(r)) - 1}{\int_M^r \gamma_n(t) \exp(-\psi(t)) dt} \int_M^x \gamma_n(t) \exp(-\psi(t)) dt + 1.$$

$M < x \leq r$ (3.16)

Because of the boundary conditions on the electron quasi-Fermi potential, electron current flows even in the absence of recombination in the interior of the transistor.

Now let us assume a recombination process that gives a recombination rate $R(n,p)$ carriers per cm^3 , then by the continuity equations

$$-\frac{d}{dx} J_p = \frac{d}{dx} J_n = R \quad (3.17)$$

If the recombination process is of Shockley-Read type, then

$$R = \frac{\exp(\varphi_p - \varphi_n) - 1}{\tau_n(p+1) + \tau_p(n+1)} \quad (3.18)$$

where the recombination center is assumed to be in the middle of the energy gap.

Now let us derive the expression for $\exp(\varphi_p(x))$ and $\exp(-\varphi_n(x))$ with carrier recombination.

From the continuity equation for holes

$$\frac{d}{dx} J_p(x) = -R$$

Integrating both sides,

$$J_p(x) = - \int_0^x R(t) dt + J_{po} \quad J_{po} = J_p(0) \quad (3.19)$$

Substituting this value of $J_p(x)$ into (3.2) and solving for

$$\frac{d}{dx} \exp(\varphi_p(x))$$

$$\begin{aligned} \frac{d}{dx} \exp(\varphi_p(x)) &= -J_p \gamma_p \exp(\psi) = - \left[- \int_0^x R dt + J_{po} \right] \gamma_p \exp(\psi) \\ &= \left[\int_0^x R dt - J_{po} \right] \gamma_p \exp(\psi) \end{aligned} \quad (3.20)$$

Integrating both sides with respect to x

$$\exp(\varphi_p(x)) = \int_0^x \left[\int_0^t R(u) du \right] \gamma_p \exp(\psi) dt - J_{po} \int_0^x \gamma_p \exp(\psi) dt + \exp(\varphi_p(0)) \quad (3.21)$$

and J_{po} can be found as

$$J_{po} = \frac{\exp(\varphi_p(0)) - \exp(\varphi_p(r)) + \int_0^r \left[\int_0^t R(u) du \right] \gamma_p \exp(\psi) dt}{\int_0^r \gamma_p \exp(\psi) dx} \quad (3.22)$$

A solution for $\exp(\varphi_n(x))$ can be obtained analogously.

$$J_n(x) = \int_0^x R dt + J_{no} \quad J_{no} = J_n(0) \quad (3.23)$$

Substituting this value of $J_n(x)$ into (3.3) and solving for

$$\frac{d}{dx} \exp(-\varphi_n(x)):$$

$$\frac{d}{dx} \exp(-\varphi_n(x)) = J_n(x) \gamma_n \exp(-\psi(x)) \quad (3.24)$$

Integrating both sides

$$\exp(-\varphi_n(x)) = \int_0^x \left[\int_0^t R(u) du \right] \gamma_n \exp(-\psi) dt + J_{no} \int_0^x \gamma_n \exp(-\psi) dt + \exp(-\varphi_n(0)) \quad (3.25)$$

$$J_{no} = \frac{\exp(-\varphi_n(r)) - \exp(\varphi_n(0)) - \int_0^x \left[\int_0^t Rdu \right] \gamma_n \exp(-\psi) dt}{\int_0^r \gamma_n \exp(-\psi) dx} \quad (3.26)$$

The result (3.25) can be generalized to the transistor problem by specifying the electron quasi-Fermi potential in two domains. In the emitter domain:

$$\exp(-\varphi_n(x)) = \int_0^x \left[\int_0^t Rdu \right] \gamma_n \exp(-\psi) dt + J_{noe} \int_0^x \gamma_n \exp(-\psi) dt + \exp(-\varphi_n(0)) \quad (3.27)$$

$0 \leq x \leq M$

with

$$J_{noe} = \frac{1 - \exp(-\varphi_n(0)) - \int_0^M \left[\int_0^x Rdu \right] \gamma_n \exp(-\psi) dx}{\int_0^M \gamma_n \exp(-\psi) dx} \quad (3.28)$$

In the collector domain:

$$\exp(-\varphi_n(x)) = \int_M^x \left[\int_M^t Rdu \right] \gamma_n \exp(-\psi) dt + J_{noc} \int_M^x \gamma_n \exp(-\psi) dt + 1. \quad (3.29)$$

$$J_{noc} = \frac{\exp(-\varphi_n(r)) - 1 - \int_M^r \left[\int_M^x Rdu \right] \gamma_n \exp(-\psi) dx}{\int_M^r \gamma_n \exp(-\psi) dx} \quad (3.30)$$

$M \leq x \leq r$

Having found the quasi-Fermi potentials we can proceed to the third step; finding a better approximation for the electrostatic potential. For this we must solve the Poisson's equation:

$$\frac{d^2\psi}{dx^2} = - \frac{q}{\epsilon\epsilon_0} (p - n + N_D^+ - N_A^-)$$

or, in normalized notation:

$$\frac{d^2\psi}{dx^2} = \exp(\psi - \varphi_n) - \exp(\varphi_p - \psi) - N \quad (3.31)$$

where $N = N_D^+ - N_A^-$ in n_i units.

This equation can be linearized by expanding to Taylor's series in terms of δ , the difference between the available trial solution and the exact solution.

$$\psi_{\text{exact}} = \psi + \delta \quad (3.32)$$

Substituting this into (3.31)

$$\frac{d^2\psi}{dx^2} + \frac{d^2\delta}{dx^2} = \exp(\psi - \varphi_n + \delta) - \exp(\varphi_p - \psi - \delta) - N(x) \quad (3.33)$$

expanding the exponential entries and keeping only the linear terms

$$\frac{d^2\psi}{dx^2} + \frac{d^2\delta}{dx^2} \approx n(1 + \delta) - p(1 - \delta) - N(x) \quad (3.34)$$

we obtain the elliptic differential equation for the difference

$$\frac{d^2\delta}{dx^2} - \delta(n + p) = \left(-\frac{d^2\psi}{dx^2} + n - p - N(x) \right) \quad (3.35)$$

The equation is of the form:

$$-\frac{d^2y}{dx^2} + u(x)y = f(x) \quad (3.36)$$

$$u(x) = n(x) + p(x)$$

$$f(x) = \psi'' - n(x) + p(x) + n(x)$$

and its solution by discrete methods are always convergent if $f(x)$ and $u(x)$ are real continuous functions and $u(x) > 0$. [23]

After discretization the system is a set of linear equations expressible in the matrix form

$$\underline{A} \cdot \underline{\delta} = \underline{v} \quad (3.37)$$

where \underline{A} is a tridiagonal matrix of the form

The solution for $\underline{\delta}$ is given by:

$$\underline{\delta} = \underline{A}^{-1} \cdot \underline{v} \quad (3.39)$$

and the improved value for the new electrostatic potential is

$$\underline{\Psi}_{\text{new}} = \underline{\Psi} + \underline{A}^{-1} \cdot \underline{v} \quad (3.40)$$

Gaussian elimination method proved to be the most effective procedure for the inversion of the matrix A. On the other hand, existing Gaussian elimination programs are extremely slow for our purpose, because of the large size of the matrix involved. Using the special character of the matrix A, a much faster and more efficient solution procedure was devised. This method also eliminates the requirement to store the whole matrix; only the diagonal elements are stored in a linear array. The mathematics of this method is explained in appendix A.

$\underline{\Psi}_{\text{new}}$ is entered as a trial solution for the next iteration, and the system is solved for new $\underline{\delta}$. If the algorithm is convergent $\|\underline{\delta}_{\text{new}}\| < \|\underline{\delta}\|$. The iteration cycle is stopped when each of the elements of $\underline{\delta}$ becomes smaller or equal to the maximum permissible error. In our calculations an error criterion of $10^{-5} \frac{kT}{q}$ was used.

The convergence of 1-D Gummel algorithm is quite satisfactory in low and moderate injection levels. This allows this algorithm to apply many physical cases with little complexity and low computer costs. We will discuss more details of this in the next chapter.

CHAPTER IV

TWO DIMENSIONAL NUMERICAL ANALYSIS -AN OVERVIEW

Today integrated circuit technology goes on its course to put more on much smaller silicon chips. Device dimensions shrink steadily, and complexity grows. Computer aided design (CAD), at this stage of development is applauded as a new productivity enhancement method in the electronics industry. Infact today's Very Large Scale Integrated (VLSI) circuits are computer simulated at the process, device, circuit and system levels to accurately predict cost and function prior to fabrication. While fabrication and actual testing is the best way to discover all the implications and limitations of any new technology, it is also the most expensive and time consuming option. A single lot of devices for a new VLSI technology cost over one million dollars to fabricate and take six months to complete. [18] Another implication of VLSI technology is that the necessity of rigid control of device parameters due to ultra small dimensions, and complexity of geometries.

In order to analyze accurately a semiconductor structure under all kinds of operating conditions, the nonlinear coupled

partial differential equations of semiconductor charge transport must be solved. Unfortunately no analytical solution exists due to nonlinearity. Therefore some numerical procedure must be employed.

In the previous chapter, we have presented a numerical procedure to solve 1-D pn junction diode and pnp transistor problems. Because of its very nature 1-D models cannot examine the lateral variations of current densities and potentials, and cannot handle semiconductor structures of special geometry. Also the variations in the threshold and the breakdown voltages due to short and narrow channel effects in MOS transistors are two and three dimensional phenomena, and cannot be analyzed by one dimensional models. [9] [13] The short channel effect reduces the threshold voltage of an n channel MOSFET. As the drain approaches the source, its positive bias raises the surface potential near the source and thus increases the amount of current flow in the device at a given gate voltage. Narrow channels have the opposite effect. [21]

The numerical problems associated with 2-D analysis are of course more challenging. The equations are partial-differential equations instead of ordinary differential equations of 1-D case.

In the following, we write these equations in a different form:

$$F_1 = \nabla^2 \psi + \frac{q}{\epsilon \epsilon_0} (p - n - N) = 0. \quad (4.1)$$

$$F_2 = \nabla \cdot [q(D_n \nabla n - \mu_n n \nabla \psi)] - q \left(\frac{\partial n}{\partial t} + R_n \right) = 0. \quad (4.2)$$

$$F_3 = \nabla \cdot [-q(D_p \nabla p + \mu_p p \nabla \psi)] + q \left(\frac{\partial p}{\partial t} + R_p \right) = 0. \quad (4.3)$$

R_n and R_p are electron and hole recombination rate densities.

Nevertheless the basic methods for solution are similar. There are two schemes to linearize these equations in either case [17]. The first is the decoupled approach, and it is sometimes called, as Gummel's algorithm. The 1-D solution procedure in chapter III is an implementation of this method. This approach solves the semiconductor equations successively in an iteration loop, so decouples them. This approach is simple to implement but it fails as the degree of coupling between the continuity equations increase as in the case of avalanche multiplication. The second linearization scheme is coupled one. In this approach the linearized equations are solved simultaneously. Both methods require an initial guess solution followed by an adjustment of the guess according to certain criteria, until an acceptable solution is obtained. While the second approach is a more general one, the numerical implementation of it on a digital computer is quite a big job. Because of this, the decoupled approach yields a more cost effective solution in many instances, and is usually preferred.

The procedure of the decoupled approach must have been understood from the previous chapter. A guess solution for electrostatic potential is entered, and, electron and hole continuity equations are solved. Then the linearized Poisson's equation is solved for a new potential. This value is returned as a guess solution for the next iteration, and so on. The iteration cycle is stopped when the required accuracy is reached. The coupled approach solves F_1 , F_2 , and F_3 simultaneously by expanding each of the equations in a Taylor series in terms of each variable. This yields the following matrix equation.

$$\begin{bmatrix} -F_1 \\ -F_2 \\ -F_3 \end{bmatrix} = \begin{bmatrix} \frac{\partial F_1}{\partial \psi} & \frac{\partial F_1}{\partial n} & \frac{\partial F_1}{\partial p} \\ \frac{\partial F_2}{\partial \psi} & \frac{\partial F_2}{\partial n} & \frac{\partial F_2}{\partial p} \\ \frac{\partial F_3}{\partial \psi} & \frac{\partial F_3}{\partial n} & \frac{\partial F_3}{\partial p} \end{bmatrix} \begin{bmatrix} \Delta \psi \\ \Delta n \\ \Delta p \end{bmatrix} \quad (4.4)$$

The coupled approach is mathematically more attractive since quadratic convergence of the solution is assured. But its development is more difficult and time consuming, and it requires more computer storage.

In all of the cases, the equations are discretized by one of the two techniques:

- a) Finite-Difference Method -FDM
- b) Finite-Element Method -FEM.

FDM is the most widely used method because of its simple implementation, but, FEM is becoming very popular with its advantages in handling irregular geometries and in economizing computer costs. [6] , [9] , [16] , [20] - [22]

Discretized differential equations result in algebraic equations expressible in the matrix form, $\underline{A} \cdot \underline{x} = \underline{b}$. The key point in any algorithm is the solution of these matrix equations. In one dimensional analysis, if the Poisson's equation is discretized on a grid of 100 points, then the resultant A matrix is 100x100. The straightforward application of an inversion technique such as Gaussian elimination is impossible. A 100x100 matrix requires a storage of 10K words, and the number of multiplications and divisions is so large that a very small diode analysis program requires hours of computer time. On the other hand, A is a sparsely but regularly populated symmetric matrix. Due its special character, more efficient inversion schemes can be devised; and by making use of the zero entries of the matrix, the storage can be reduced drastically.

In higher dimensional simulation, the problem is much more severe. The current continuity equations cannot be solved by direct integration anymore, they must be solved by discrete

techniques like Poisson's equation. [8] If the equations are discretized on a mesh of N nodes, then we have three $N \times N$ matrices. N can be as large as 1000 and 2000. If the coupled method is employed, we obtain one matrix of size $3N \times 3N$. It is seen that the storage of the coupled method is three times larger than the decoupled approach.

The use of direct inversion techniques -whether improved or as crude as Gaussian elimination- is impossible, and so-called iterative techniques are utilized in this task. The choice of the iterative technique is another problem; and we will devote the next section to this topic; the most important problem in the numerical solution of differential equations.

Solution of matrix equations by iterative methods:

Semiconductor equations under steady state conditions are elliptic equations of space. In the following we shall give an example of how an elliptic equation is discretized by FDM, and we shall discuss its solution by some simple iterative methods.

Consider one of the simplest cases: Laplace's equation in the square ζ $0 < x < 1$, $0 < y < 1$

$$\nabla^2 V = \frac{\partial^2 V}{\partial x^2} + \frac{\partial^2 V}{\partial y^2} = 0. \quad (4.5)$$

and $V(x,y)$ satisfies the Dirichlet boundary conditions $V = \phi(x,y)$ a known function along the boundary of the square ζ .

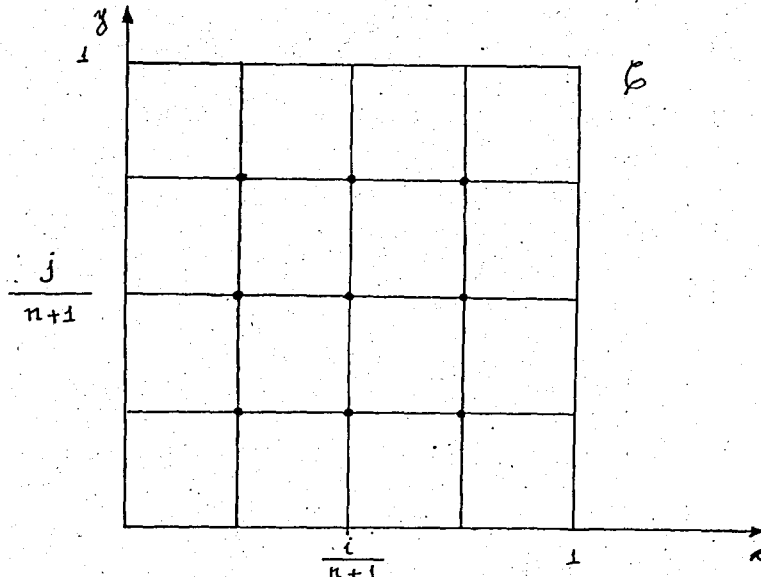


Fig.4.1

The method of finite differences consists of dividing the sides of the square into $n+1$ parts, giving the grid points

$$P_{ij} = (x_i, y_j) \text{ where, for example } x_i = \frac{i}{n+1} \text{ and}$$

$$y_j = \frac{j}{n+1} \quad i=0,1,\dots,n+1 \quad ; \quad j=0,1,\dots,n+1$$

The interior points are those which correspond to $i=1,2,\dots,n$ and $j=1,2,\dots,n$. Write $V_{ij} = V(x_i, y_j)$. Then we are required to determine V_{ij} so that

$$\frac{V_{i+1,j} - 2V_{ij} + V_{i-1,j}}{h^2} + \frac{V_{i,j+1} - 2V_{ij} + V_{i,j-1}}{h^2} = 0. \quad (4.6)$$

if P_{ij} is an interior point of the square; and $V_{ij} = i_j$ if P_{ij} is on the boundary. Here we have written $h = \frac{1}{n+1}$.

Arranging

$$V_{i,j+1} + V_{i,j-1} + V_{i+1,j} + V_{i-1,j} + 4V_{ij} = 0. \quad (4.7)$$

We can write (4.7) in a number of ways; it is only necessary to arrange the interior points P_{ij} in a sequence. For example we may take the order

$$P_{11}, P_{21}, \dots, P_{n1}, P_{12}, \dots, P_{n2}, \dots, P_{1n}, \dots, P_{nn}$$

and let $X_k = V_{ij}$ with $k = n(j-1) + i \quad k=1,2,\dots,n^2$

We have obtained the system of equations of the discretized system. Now let us see how we can solve them.

The principle of any iterative method for the solution of $\underline{A} \cdot \underline{x} = \underline{b}$ is to find an initial guess \underline{x}_0 and calculate the corresponding residual $\underline{r}_0 = \underline{A} \cdot \underline{x}_0 - \underline{b}$, and then modify \underline{x}_0 , calculate the new residual, and so on. The process is stopped when the residual falls below the permissible error.

The two sequences of vectors obtained in this process:

$$\{x_1, x_2, \dots, x_p, \dots\}$$
$$\{y_1, y_2, \dots, y_p, \dots\}$$

How do we obtain the new solution vector from the previous one and its corresponding residual?

$$\text{Let } \underline{x}_p = \begin{bmatrix} \epsilon_1^p \\ \epsilon_2^p \\ \vdots \\ \vdots \\ \vdots \\ \epsilon_n^p \end{bmatrix} \quad \text{and } \underline{r}_p = \underline{A} \cdot \underline{x}_p - \underline{b} = \begin{bmatrix} \rho_1^p \\ \rho_2^p \\ \vdots \\ \vdots \\ \vdots \\ \rho_n^p \end{bmatrix}$$

Take the i th equation

$$a_{i1}x_1 + \dots + a_{in}x_n = b_i$$

and replace

$$\begin{bmatrix} x_1 \\ x_2 \\ \vdots \\ x_{j-1} \\ x_{j+1} \\ \vdots \\ x_n \end{bmatrix} \quad \text{by} \quad \begin{bmatrix} \xi_1^p \\ \xi_2^p \\ \vdots \\ \xi_{j-1}^p \\ \xi_{j+1}^p \\ \vdots \\ \xi_n^p \end{bmatrix}$$

We obtain one equation in the single unknown x_j . We can solve this provided $a_{ij} \neq 0$.

$$x_j = \frac{1}{a_{ij}} \left(b_i - \sum_{k \neq j} a_{ik} \xi_k^p \right) \quad (4.10)$$

This value is equal to

$$\xi_j^{p+1} = \xi_j^p - \frac{\beta_i^p}{a_{ij}} \quad (4.11)$$

since

$$\beta_i = \sum_1^n a_{ik} \xi_k^p - b_i \quad (4.12)$$

Now we define the vector

$$x_{p+1} = \begin{bmatrix} \xi_1^{p+1} \\ \vdots \\ \xi_n^{p+1} \end{bmatrix}$$

where $\xi_i^{p+1} = \xi_i^p$ for $i \neq j$ and ξ_j^{p+1} has the value given by (4.10).
Then clearly $\rho_i^{p+1} = 0$.

Thus we have defined the vector x_{p+1} having all its components except one (the j th) the same as those of x_p , and this one chosen so that one of the equations, the i th has a zero residual. This is therefore a means of defining x_{p+1} in terms of x_p . We must now consider the question of the choice of particular values of i (the residual to be reduced to zero) and of j (the component to be altered).

Southwell's method:

Choice of equation : i is so chosen that

$$|\rho_i^p| = \text{Max}_k |\rho_k^p|$$

i.e we relax the equation for which the residual has the largest absolute value. If there are several values of i for which the maximum is attained, we might take the largest i .

Choice of component: choose $j=i$, (diagonal elements assumed to be all nonzero).

- i) choose i so that $|\rho_i^p|$ is maximum.
- ii) $\xi_k^{p+1} = \xi_k^p$ for $k \neq i$
- iii) $\xi_i^{p+1} = \xi_i^p - \rho_i^p / a_{ii}$

Number of operations:

In each step we must :

- 1) Given the ρ_i^p , compute the ξ_i^{p+1} . this only requires one division and addition.

2) Calculate the new ρ_i^{P+1} . Since

$$\rho_j^{P+1} = -b_j + \sum_{k=1}^n a_{jk} \xi_k^{P+1} = -b_j + \sum_{k=1}^n a_{jk} \xi_k^P - a_{ji} \xi_i^P + a_{ji} \left(\xi_i - \frac{\rho_i}{a_{ii}} \right) \quad (4.13)$$

we have

$$\rho_j^{P+1} = \rho_j^P - a_{ji} \rho_i^P / a_{ii} \quad (4.14)$$

This requires $n-1$ multiplications and $n-1$ additions. Approximately $n^2/3$ cycles of this process correspond to the same amount of labor as the Gaussian elimination process.

The Gauss-Seidel Method:

Choice of equation: Equations are chosen in cyclic order.

1,2,3,.....,n,1,2,.....

Choice of component : As in Southwell's method we take $j=i$. The step from x_p to x_{p+1} is then given by

i) i = remainder on division of $p+1$ by n , or n if this is zero.

ii) $\xi_k^{P+1} = \xi_k^P$ if $k \neq i$

iii) $\xi_i^{P+1} = \xi_i^P - \rho_i^P / a_{ii}$

The number of operations in each step is the same as in Southwell's method, and the residuals are given by the same formula

$$\rho_j^{P+1} = \rho_j^P - a_{ji} \rho_i^P / a_{ii} \quad j=1,2,\dots,n$$

This process converges faster than Southwell's method,

and has the advantage of being more automatic which facilitates programming.

Successive over-relaxation method:

This is another method involving the relaxation of a single component, in the same way as the Gauss-Seidel method.

- 1) As before we choose the equations in cyclic order.
- 2) We alter the i th component in the i th step as follows.

$$\text{If } \underline{x}_p = \begin{bmatrix} \xi_i^{(p)} \end{bmatrix}, \quad \underline{x}_{p+1} = \begin{bmatrix} \xi_i^{(p+1)} \end{bmatrix}$$

we modify x_p into x_{p+1} by writing

$$\begin{aligned} \xi_k^{(p+1)} &= \xi_k^{(p)} && \text{if } k \neq i \\ \xi_i^{(p+1)} &= \xi_i^{(p)} + \omega (\tilde{\xi}_i^{(p+1)} - \xi_i^{(p)}) \\ &= (1 - \omega) \xi_i^{(p)} + \omega \tilde{\xi}_i^{(p+1)} \end{aligned}$$

(4.15)

Here ω is a constant called the over-relaxation factor and is nonzero. If $\omega = 1$ SOR method is equivalent to the Gauss-Seidel method. There is a lot of theory on the determination of optimum ω for the fastest convergence rate. The SOR method diverges for $\omega > 2$. So $1 \leq \omega < 2$.

SOR method is the most commonly used method for iterative solution of linear matrix equations. All the iteration methods

we have counted so far are point iterative methods, because they are based on the relaxation of only one component. After 1960's block or iterative methods with reportedly superior convergence rate have been developed. (e.g. SLOR-successive line over-relaxation). It has been shown that by reversing the cyclic ordering or by alternating it, one can improve convergence. Usually user by experimenting, might find the best scheme which suits his particular application. Nowadays (1983) block-iterative methods or Stone's method [29] are usually employed if direct solvers cannot be used.

CHAPTER V

MINIMOS PROGRAM- A TWO DIMENSIONAL MOS TRANSISTOR ANALYZER

MINIMOS, a program developed at Technical University of Vienna is a general purpose user oriented CAD tool which can be used to analyze MOS transistor under steady state conditions.

[19] It is written in ANSI 77 FORTRAN.

Minimos is a two dimensional Gummel Algorithm-i.e it uses the decoupled approach. The unique feature of the program is its dynamic mesh refreshment. The mesh on which the equations are discretized is regenerated at each iteration to improve convergence rate and dynamically adjust the storage.

Recombination which is not very important in MOS transistors is neglected. The mobility model is also original. The mobility is assumed to be a function of temperature (T), the electric field component parallel to the current flow (E_p), the electric field component perpendicular to the Si-SiO₂ interface, (E_T), the distance to this interface (y), the concentration of impurities N , and the mobile carrier density (n or p)

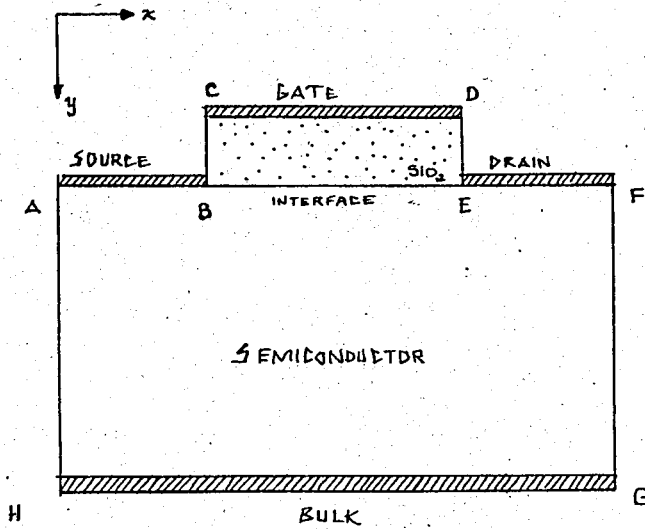


Fig.5.1

Electron mobility is expressed as

$$\mu_n(T, E_p, E_T, y, N, n) = \left(\frac{1}{\mu_{LI}^\beta} + \frac{1}{\mu_{EBET}^\beta} \right)^{1/\beta} \quad (5.1)$$

$$\beta = 2.57 \times 10^{-2} \cdot T^{.66} \quad [30] \quad (5.2)$$

μ_{LI} describes the influence of lattice scattering, impurity scattering, and screening as a function of temperature. Thus

$$\mu_{LI} = \mu_{LI}(T, N, n) \quad (5.3)$$

μ_{EBET} describes the influence of velocity saturation and surface scattering as a function of temperature and the distance to the Si-SiO₂ interface. Thus

$$\mu_{EBET} = \mu_{EBET}(T, E_p, E_T, y) \quad (5.4)$$

μ_{LI} is constructed from two components; where μ_L denotes the pure lattice mobility as a function temperature and μ_I denotes the impurity scattering mobility.

$$\mu_L = 7.12 \times 10^8 \cdot T^{-2.3} \quad (\text{cm}^2/\text{V.s}) \quad (5.5)$$

$$\mu_I = \frac{7.13 \times 10^{17} \cdot T^{1.5}}{N \cdot f\left(\frac{1.52 \times 10^{15} \cdot T^2}{n}\right)} \quad (5.6)$$

where $f(x) = \ln(1+x) - \frac{x}{1+x}$

These two mobility components are merged by a formula first given by Debye [31]

$$\mu_{LI} = \mu_L \left[1 + g\left(\left(\frac{6\mu_L}{\mu_I}\right)^{1/2}\right) \right] \quad (5.7)$$

with $g(x) = x^2 \left(\text{Ci}(x) \cos x + \sin x \left(\text{Si}(x) - \frac{\pi}{2} \right) \right)$ (5.8)

$$\text{Ci}(x) = - \int_x^\infty \frac{\cos t}{t} dt = C + \ln x + \int_0^x \frac{\cos t - 1}{t} dt$$

$$\text{Si}(x) = - \int_x^\infty \frac{\sin t}{t} dt = - \frac{\pi}{2} + \int_0^x \frac{\sin t}{t} dt \quad [33]$$

μ_{EPET} is also built from two parts, where μ_{EP} describes the influence of velocity saturation and μ_{ET} models surface scattering.

$$\mu_{EP} = \frac{1.53 \times 10^9 T^{-.87}}{-E_P} \cdot \left(\frac{y + 10^{-7}}{y + 2 \times 10^{-7}} \right) \quad (\text{cm}^2/\text{V.s}) \quad (5.9)$$

$$\mu_{ET} = 10^8 (y + 2 \times 10^{-7})^{1/2} \cdot h(E_T)^{-1/2} \quad (5.10)$$

with $h(x) = x + (x)^{1/2}$

These two parts are combined empirically with a Mathiessens rule with weight 2

$$\mu_{EPET} = \left(\frac{1}{\mu_{EP}^2} + \frac{1}{\mu_{ET}^2} \right)^{-1/2} \quad (5.11)$$

The formulas for hole mobility are identical in mathematical structure

$$\mu_p (T, E_p, E_T, y, N, p) = \left(\frac{1}{\mu_{LI}^\beta} + \frac{1}{\mu_{EPET}^\beta} \right)^{-\frac{1}{\beta}} \quad (5.12)$$

$$\beta = .46 T^{.17}$$

$$\mu_L = 1.35 \times 10^8 T^{-2.2} \quad (\text{cm}^2/\text{V.s}) \quad (5.13)$$

$$\mu_I = \frac{5.6 \times 10^{17} T^{1.5}}{N.f \left(\frac{2.5 \times 10^{15} T^2}{p} \right)} \quad (\text{cm}^2/\text{V.s}) \quad (5.14)$$

$$\mu_{LI} = \mu_L \left(1 + g \left(\left(\frac{6\mu_L}{\mu_I} \right)^{1/2} \right) \right) \quad (5.15)$$

$$\mu_{EP} = \frac{1.62 \times 10^8 T^{-.52}}{E_p} \left(\frac{y + 2 \times 10^{-7}}{y + 4 \times 10^{-7}} \right)^{1/2} \quad (\text{cm}^2/\text{V.s}) \quad (5.16)$$

$$\mu_{ET} = 2.6 \times 10^8 (y + 4 \times 10^{-7}) \cdot h(-E_T)^{-1/2} \quad (\text{cm}^2/\text{V.s}) \quad (5.17)$$

$$\mu_{EPET} = \left(\frac{1}{\mu_{EP}^2} + \frac{1}{\mu_{ET}^2} \right)^{-1/2} \quad (5.18)$$

The functions f,g,h are identical in structure in each case.

Boundary conditions:

In oxide region Poisson's equation reduces to Laplace's equation

$$\nabla^2 \psi = 0. \quad (5.19)$$

At the contacts (AB:Source,CD:Gate,EF:Drain,GH:Bulk,see Fig.5.1) which are assumed to be ohmic, the potential is kept constant to the applied voltage plus the appropriate built-in voltage caused by the doping.

At the Si-SiO₂ interface

$$\left[\epsilon_{ox} \frac{\partial \psi}{\partial y} \right]_{ox} = \left[\epsilon_{si} \frac{\partial \psi}{\partial y} \right]_{si} \quad (5.20)$$

At the vertical boundaries (AH,CB,DE,FG) the lateral electric field has to vanish.

At the source contact (AB) and the drain contact (EF) the carrier density is kept constant to the value of doping concentration.(Thermal equilibrium exists.) At the interface (BE) no current component in the y-direction is allowed. At the vertical boundaries (AH,FG) the lateral current component has to vanish. At the bulk contact (HG) no current components are allowed.

The matrix equations are solved by an iterative technique called by SIP method [29] which is found to be superior to existing block iterative techniques. [19]

The MINIMOS program can calculate the doping profile by a process modeling program SUPREM. [15] The vertical profiles of SUPREM are fitted in the lateral direction. The doping profile may be specified also by the user point by point. This approach, despite the complication caused, offers the practicability to simulate complex structures. SUPREM allows us to find the impurity profiles by diffusion and ion implantation together with the annealing process. With all of these, MINIMOS is a complete device simulation program, from fabrication to circuit behavior.

CHAPTER VI

DISCUSSION OF RESULTS AND CONCLUSION

Here we present some of the results obtained by one-dimensional diode and transistor analysis.

I - Analysis of a lightly doped pn-junction

$$N_A = 10^{16} \text{ cm}^{-3} \quad N_D = 10^{15} \text{ cm}^{-3}$$

$$V_{\text{bias}} = 0.5 \text{ volt} \quad \text{temperature} = 25^\circ\text{C.}$$

Under these conditions a diode current of $I_d = 1.65 \times 10^{-3} \text{ A}$ flows with a crosssectional area of 0.001 cm^2 .

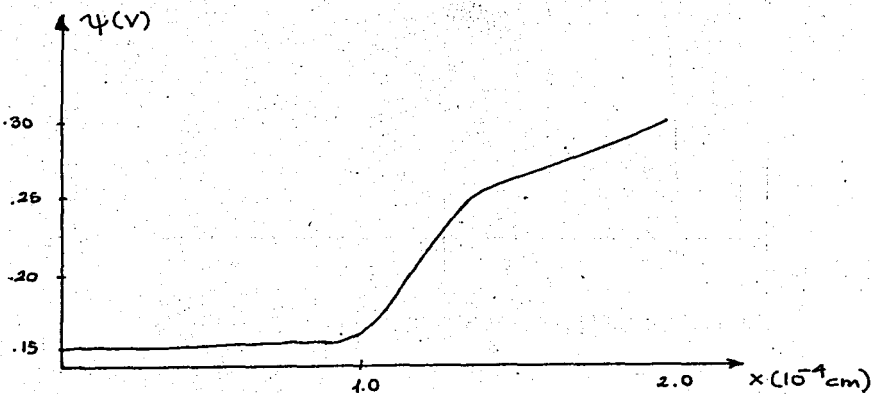


Fig.6.1 Electrostatic potential

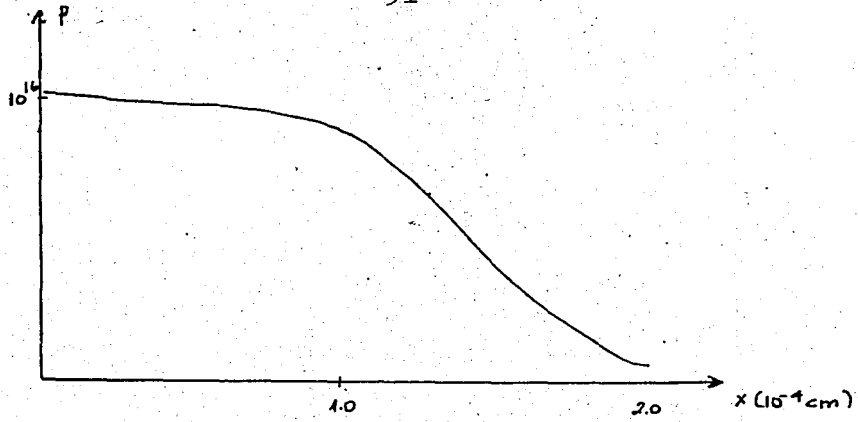


Fig.6.2 Hole concentration

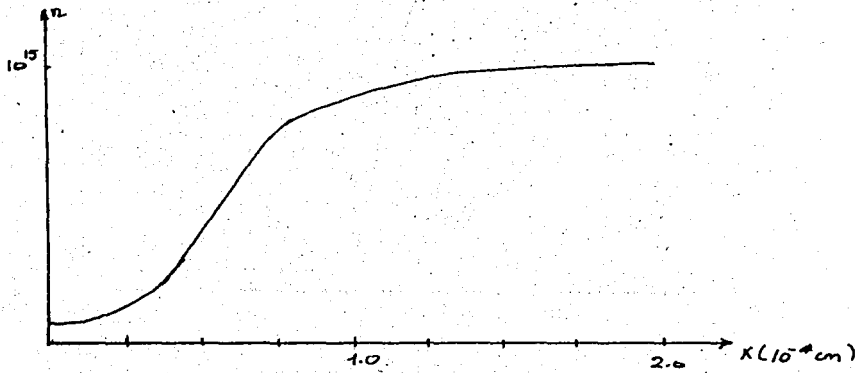


Fig.6.3 Electron concentration

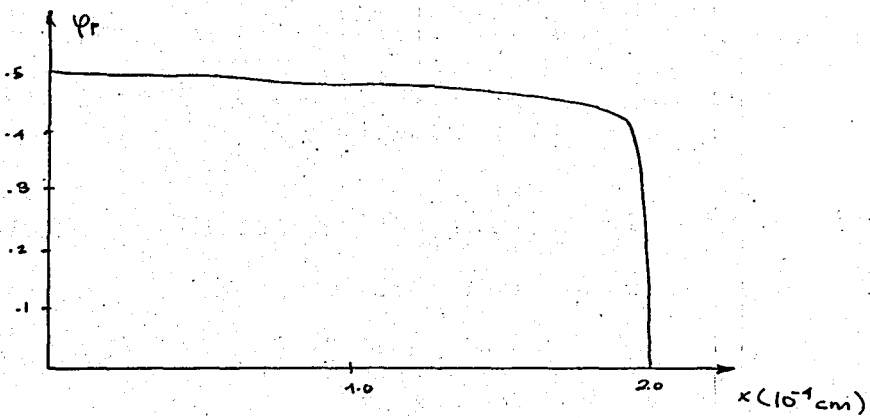


Fig.6.4 Hole quasi-Fermi potential

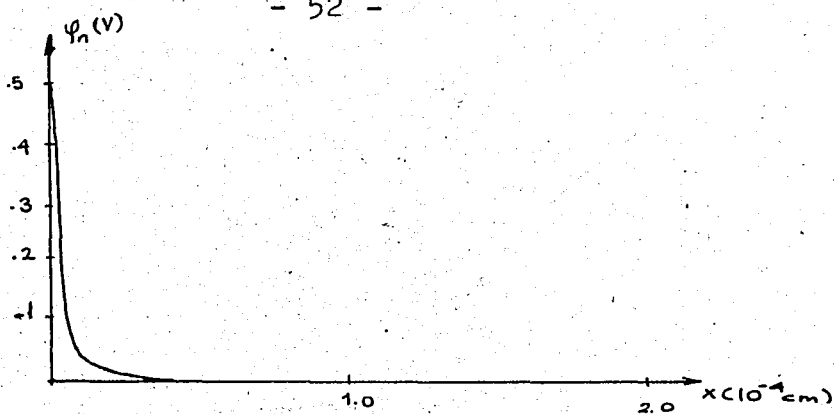


Fig.6.5 Electron quasi-Fermi potential

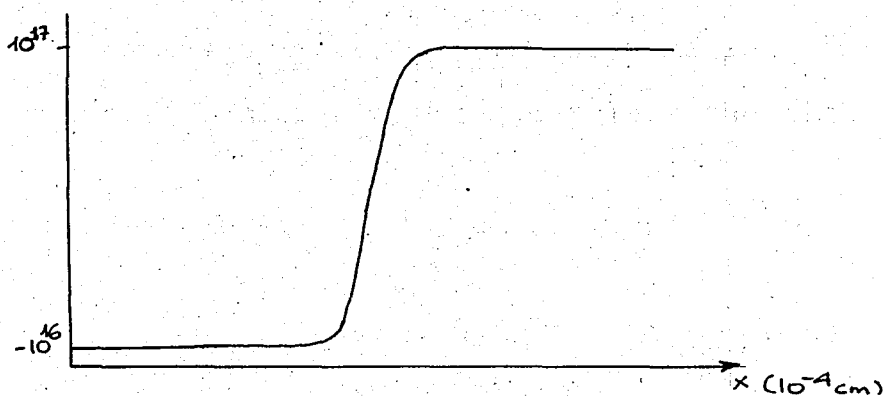


Fig.6.6 Doping profile

The abruptness of the junction is smoothed by the step approximating function $\frac{1}{1+\exp(-b(x-x_0))}$ $b > 0$

The DIODE program reaches to this results in 4 iterations. Bias voltage, doping concentration and temperature are the major factors governing the convergence rate.

The same junction is reverse biased by 0.2volts

$$V_{\text{bias}} = -0.2 \text{ volts}$$

$$I_d = -3.3 \times 10^{-11} \text{ amperes}$$

$$\text{no. of iterations} = 4$$

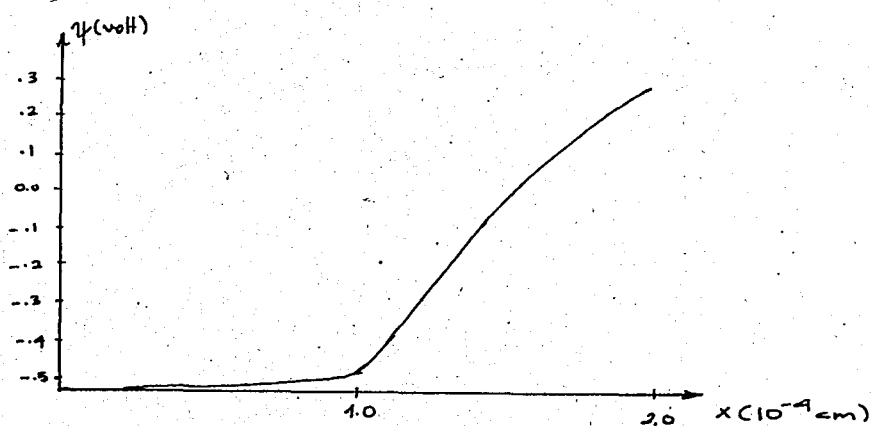


Fig.6.7

The linear change of potential in the n-region indicates that this region is depleted of free carriers (the lightly doped section).

Now let us see the effect of temperature

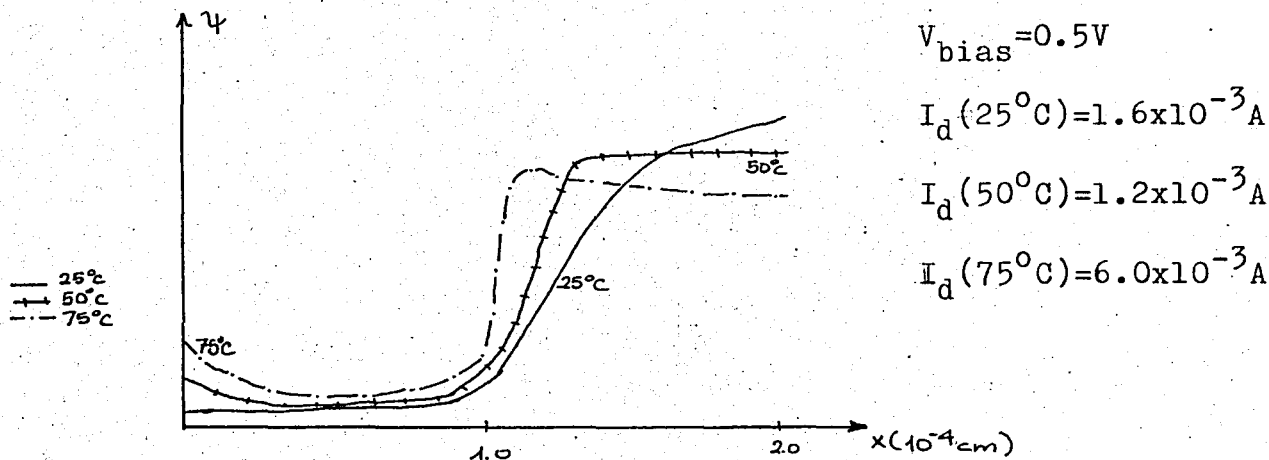


Fig.6.8 Decreasing barrier height with increasing temperature

II- pn^+ junction

$$N_A = 10^{15} \text{ cm}^{-3} \quad N_D = 10^{19} \text{ cm}^{-3}$$

$$V_{\text{bias}} = 0.3 \text{ volts} \quad \text{temperature} = 25^\circ C.$$

no. of iterations = 44

$$I_d = 2.2 \times 10^{-5} A$$

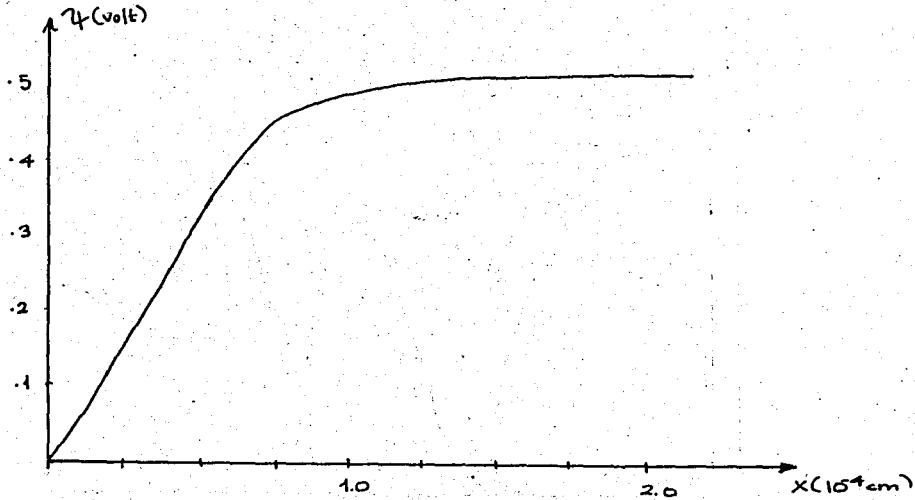


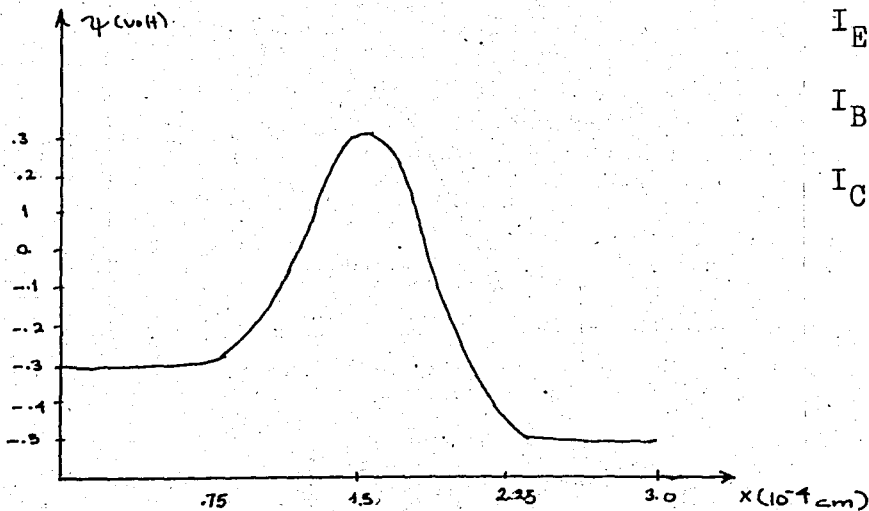
Fig.6.10

The scheme becomes divergent if the doping densities pass the border of 10^{19} cm^{-3} . As Maxwell-Boltzmann distribution is used in this analysis, this marks the upper limit that this approximation is valid.

III- pnp transistor

$$N_{AE} = 10^{17} \quad N_{DB} = 10^{16} \quad N_{AC} = 10^{17}$$

$$V_{eb} = .1 \text{ volt} \quad V_{cb} = -.1 \text{ volt}$$



$$I_E = 7.08 \times 10^{-12} \text{ A}$$

$$I_B = -8.9 \times 10^{-15} \text{ A}$$

$$I_C = 7.08 \times 10^{-12} \text{ A}$$

Fig.6.11

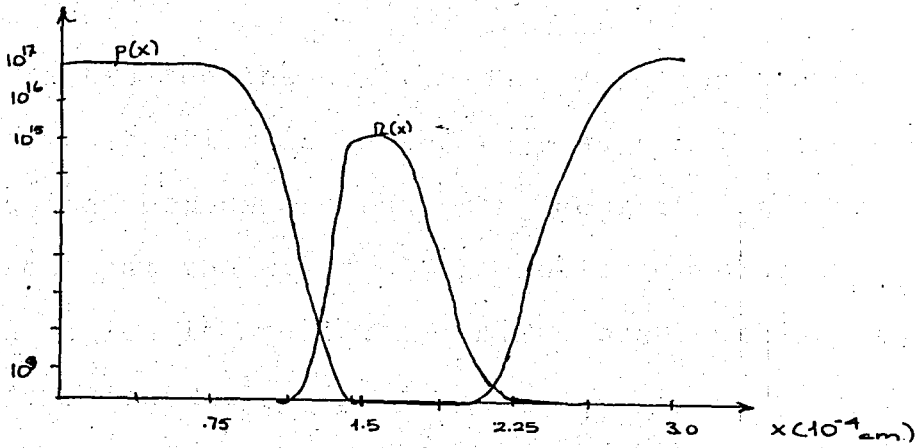


Fig.6.12

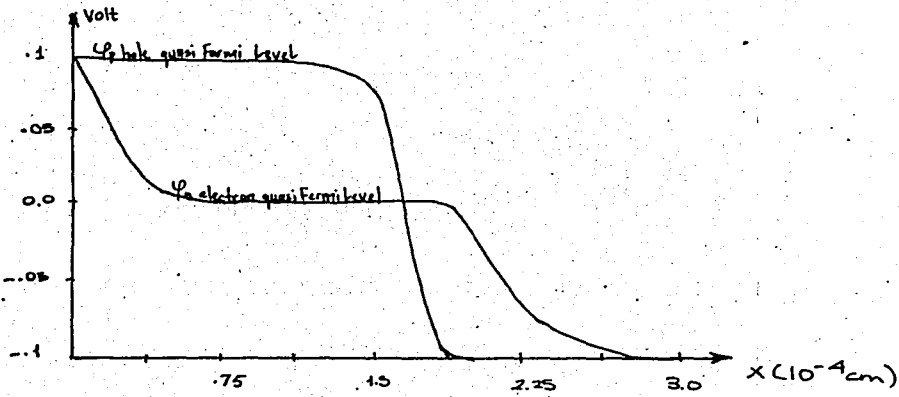


Fig.6.13

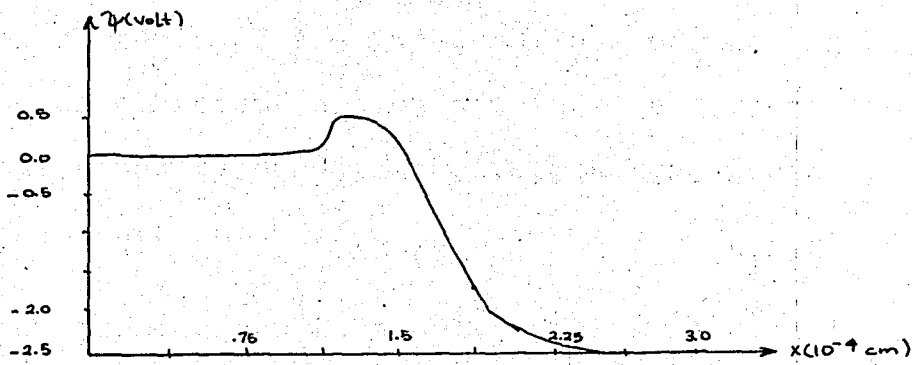


Figure.6.14. -Same transistor with $V_{eb} = .5\text{V}$ and $V_{cb} = -2\text{V}$.

Forward bias on the emitter-base junction decreases the height of the barrier, while the reverse bias on the collector-base junction deepens the potential downhill at this junction. Also, we see that the width of the collector-base junction depletion region is modulated (so, the basewidth) by the bias on this junction (Early effect).

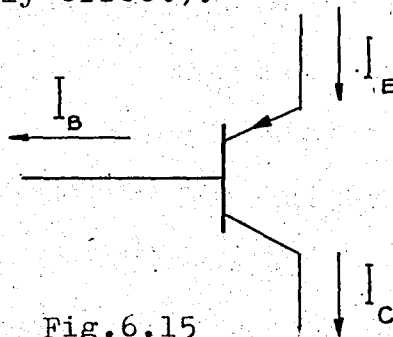


Fig.6.15

The current references used in this analysis are indicated in Fig.6.15. Since we ignored the recombination of carriers, we cannot talk of the classical transistor parameters α and β . In this case, the base current is not the amount of emitter current not collected by the collector, but the sum of the saturation currents of the two junctions of the transistor. Even in the absence of recombination an electron current flows to satisfy the boundary conditions, i.e., thermal equilibrium

$$n(0) = n_i^2 / N_{AE} \qquad n(r) = n_i^2 / N_{AC}$$

Recombination can be easily incorporated in this program according to the method established in chapter III. Breakdown of reverse biased junctions can be analyzed by adding an avalanche multiplication term to the continuity equations.

$$\xi_I = \frac{1}{q} (\alpha_n(E) |J_n| + \alpha_p(E) |J_p|) \quad (6.1)$$

$$\alpha_n(E) = 2.25 \times 10^7 \exp(-3.2 \times 10^6/E)$$

$$\alpha_p(E) = 3.80 \times 10^6 \exp(-1.75 \times 10^6/E) \quad [2]$$

One of the problems encountered in the numerical analysis of semiconductor devices is the wide range of the values of the parameters involved. Dimensions of the order of microns and atomic densities up to 10^{20} are side by side. Exponentiation of large numbers may cause overflow and the exponentiation of large negative numbers causes underflow. For this reason, some sort of normalization is necessary.

Any numerical algorithm tested for convergence must be tested first, by equating all constants to 1. After the method is proved to work the numbers are replaced with suitable normalization. 1-D methods are the starting point of any new algorithm to be tested.

These programs may be fitted to work with programs that calculate the resultant doping profile according to the given process. Suprem II is such a process engineering modeling program, and it can compute the doping profiles obtained by diffusion and ion implantation.

The Minimos program is written in ANSI 77 FORTRAN. FTN 8R1 the fortran compiler on Boğaziçi University Univac 1106 system is a subset of ANSI 77 FORTRAN. The missing features of the

compiler is completed by the subprograms written in both assembly language and fortran. Despite these efforts the program still has not been run successfully on Univac system. The problems are expected to be solved with the new CDC system since Minimos is originated on a CDC Cyber 75 system at Technical University of Vienna.

The revenues of simulation programs are most derived when the program is fitted to a graphics package and high resolution graphics. Also the results obtained through computation must be checked versus the experimentally measured values to prove the validity of the numerical method.

APPENDIX A

Mathematics of 1-D diode and transistor analysis:

Discretization: Derivatives are approximated by differences; integrals are approximated as sums.

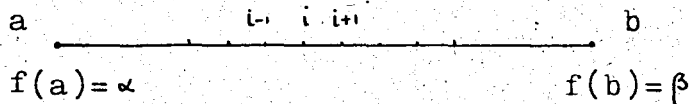
$$f'(x) = \frac{f(x) - f(x-h)}{h} \quad h \text{ sufficiently small} \quad (\text{A.1})$$

$$f''(x) = \frac{f'(x) - f'(x-h)}{h} = \frac{f(x) - 2f(x-h) + f(x-2h)}{h^2}$$

This discretization is called backward Euler approximation for derivatives.

In elliptic differential equations no first order derivatives exist. In our analysis, we used the central differences for the second derivatives for easy treatment of the boundary points.

$$f''(x) = \frac{f(x+h) - 2f(x) + f(x-h)}{h^2} \quad (\text{A.2})$$



This value of x_n is substituted in the n-1st equation.

$$a_{n-1,n-1} \cdot x_{n-1} - x_n = b_{n-1}$$

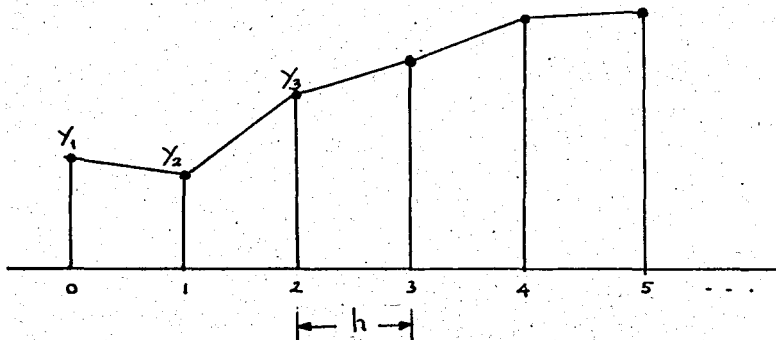
$$x_{n-1} = \frac{b_{n-1} + x_n}{a_{n-1,n-1}} \quad (\text{A.10})$$

Continuing this process we obtain the general back substitution formula:

$$x_{i-1} = \frac{b_{i-1} + x_i}{a_{i-1,i-1}} \quad i = n, n-1, \dots, 2 \quad (\text{A.11})$$

Evaluation of $\exp(\varphi_p(x))$

$$\exp(\varphi_p(x)) = \frac{\exp(\varphi_p(r)) - \exp(\varphi_p(0))}{\int_0^r \gamma_p(t) \exp(\psi(t)) dt} \int_0^x \gamma_p(t) \exp(\psi(t)) dt + \exp(\varphi_p(0)) \quad (\text{A.12})$$



The integrals are approximated by sums. Trapezoidal rule was selected because of simplicity in implementation and speed.

$$F_i = \frac{Y_i + Y_{i-1}}{2} \cdot h + F_{i-1} \quad (\text{A.13})$$

with $h = x_{i+1} - x_i$

and $F_0 = 0$.

APPENDIX B

Calculation of guess solutions for DIODE and PNP programs

The guess solution is calculated by a subroutine named GUESOL. Although these subroutines have the same name, the GUESOL of the transistor problem is different from that of DIODE.

Actually these subroutines compute the potential distribution according to Shockley's theory. The potential does not change in the bulk but in the space charge regions. In other words, electric field is zero outside the space charge regions.

In the following we discuss the calculation of guess solution for the transistor, since the diode is just a simple case of the first.

Potential at the end points (emitter and collector) are calculated as:

$$\psi(o) = V_{EB} - \frac{kT}{q} \ln(\sqrt{(N(o)/2)^2 + 1} - N(o)/2) \quad (B.1)$$

$$\psi(r) = V_{CB} - \frac{kT}{q} \ln(\sqrt{(N(r)/2)^2 + 1} - N(r)/2) \quad (B.2)$$

The potential barrier at the base emitter junction is:

$$\phi_{BE} = \frac{kT}{q} \ln\left(\frac{N_{AE}N_{DB}}{n_i^2}\right) \quad (B.3)$$

N_{AE} : average density of acceptors in the emitter region.

N_{DB} : average density of donors in the base region.

The base-collector potential difference(barrier) is:

$$\phi_{BC} = \frac{kT}{q} \ln\left(\frac{N_{AC}N_{DB}}{n_i^2}\right) \quad (B.4)$$

N_{AC} : average density of acceptors in the collector.

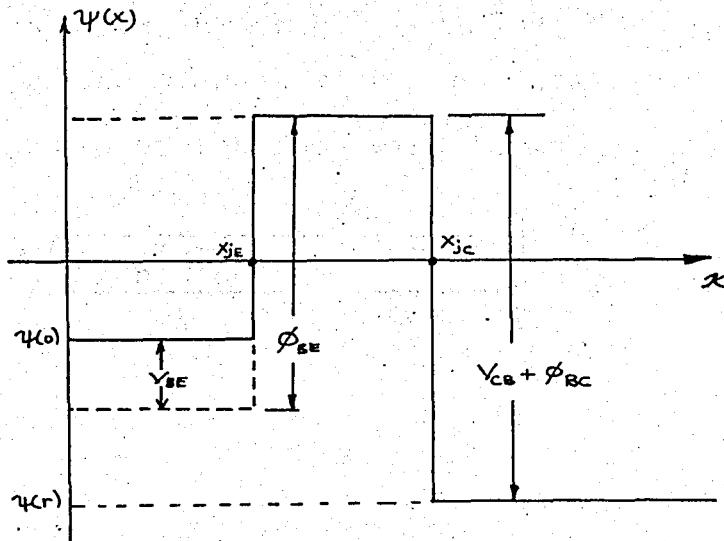


Fig.B.1

The potential distribution in Fig.C.1 cannot be used for computations because of the discontinuities at the junctions. By assuming linear change of potential across the depletion regions, this solution can be refined.

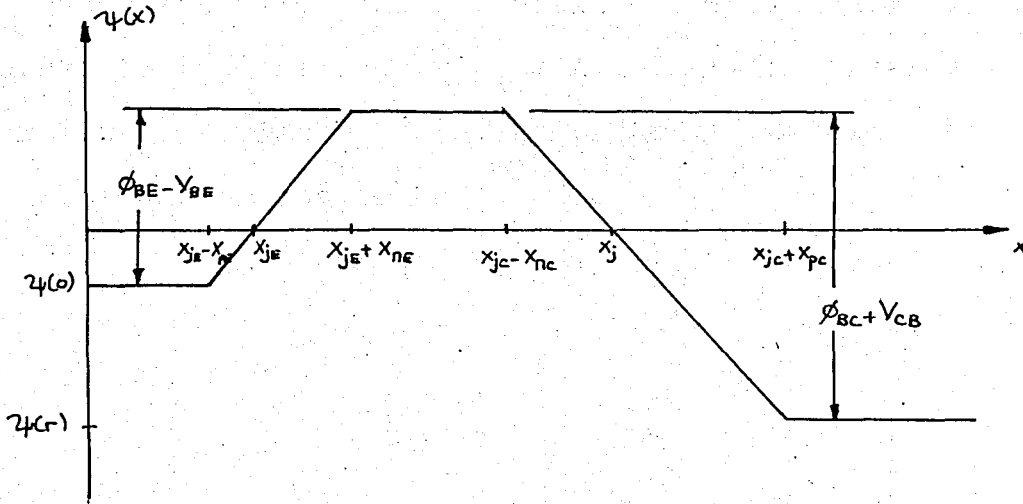


Fig.B.2

x_p and x_n are the extent that the depletion region penetrates to the p and n sides respectively. They are calculated by the use of the following formulas.

$$x_p = \sqrt{\frac{2\epsilon_r \epsilon_0 (\phi_0 - V)}{q} \cdot \frac{N_D}{N_A(N_A + N_D)}} \quad (B.5)$$

$$x_n = \sqrt{\frac{2\epsilon_r\epsilon_0(\phi_0 - V)}{q} \cdot \frac{N_A}{N_D(N_A + N_D)}} \quad (\text{B.6})$$

The guess solutions so obtained are discretized and returned to the calling program. Although the treatment is in unnormalized variables here, the programs work with variables normalized according to Table 3.1.

REFERENCES

- 1) H.K. Gummel, "A self-consistent iterative scheme for one-dimensional transistor calculations," IEEE Trans. Electron Devices, vol. ED-11, pp 455-465, 1964.
- 2) D.L. Scharfetter and H.K. Gummel, "Large-signal analysis of a silicon Read diode oscillator," IEEE Trans. Electron Devices, vol. ED-16, pp 64-77, 1969.
- 3) A. van der Ziel, "Solid state physical electronics", Prentice-Hall Inc., Englewood cliffs, N.J., 1968.
- 4) J.P. McKelvey, "Solid state and semiconductor physics", Harper and Row, 1969.
- 5) D. Vandorpe et al. "An accurate two dimensional numerical analysis of the MOS transistor," Solid state electronics, vol. 15 pp 547-557, 1972.
- 6) J. Barnes and J. Lomax, "Two-dimensional finite-element simulation of semiconductor devices", Electronics Letters, vol. 10, no. 16, pp 341, 343, 1974.
- 7) M.S. Mock, "A two-dimensional mathematical model of the insulated-gate field-effect transistor, Solid-State Electronics, vol. 16 pp 601-609, 1973.

- 8) J.W. Slotboom, "Computer-aided two-dimensional analysis of bipolar transistors", IEEE Trans. Electron Devices, vol. ED-20, no.8, pp 669-679, 1973.
- 9) P.E. Cottrell, E.W. Buturla, "Steady state analysis of field effect transistors via the finite element method", special reprint of paper, IBM corp.
- 10) H.H. Heimeier, "A two-dimensional numerical analysis of a silicon npn transistor", IEEE Trans. Electron Devices, vol. ED-20, no.8, pp 708-714, 1973.
- 11) M. Reiser, "A two-dimensional numerical FET model for dc, ac and large signal analysis", IEEE Trans. Electron Devices, vol. ED-20, no.1, pp 35-45, 1973.
- 12) V. Alwin, D.H. Navon, L.J. Turgeon, "Time dependent carrier flow in a transistor structure under non-isothermal conditions, IEEE Trans. Electron Devices, vol. ED-24, no.11, pp 1297-1304, 1977.
- 13) T. Toyabe, S. Asai, "Analytical models of threshold voltage and breakdown voltage of short-channel MOSFET's derived from two dimensional analysis", IEEE Trans. Electron Devices, vol. ED-26 no.4, pp 453-460, 1979.
- 14) D.J. Chin and D.H. Navon, "Two-dimensional analysis of the interdigitated back-contact solar cell", Solid State Electronics, vol.26, pp 104-114, 1980.
- 15) D.A. Antoniadis, S.E. Hansen, R.W. Dutton, "SUPREM II - A program for Ic process modeling and simulation", Stanford Electronics Lab. Technical Report No.5019-2, 1978.

- 16) Y. Matsuda, "Survey for the numerical analysis of semiconductors", CS742a seminar notes, IBM Corp., 1980.
- 17) E. M. Buturla, "Linearization Methods", in "An introduction to the numerical analysis of semiconductor devices and integrated circuits", lecture notes of a short course in NASECODE II conference, pp 16-21, 1981.
- 18) P. E. Cottrel, "engineering aspects-utility of application", *ibid.* pp 26-28.
- 19) S. Selberherr, A. Schütz, H. W. Pötzl, "MINIMOS-A two dimensional MOS transistor analyzer", IEEE Trans. Electron Devices, vol. ED-27 no. 8, pp 1540-1549, 1980.
- 20) B. T. Browne and J. J. H. Miller, eds, "Numerical analysis of semiconductor devices and integrated circuits," Proceedings of the NASECODE II Conference, Dublin, 1981.
- 21) E. M. Buturla, P. E. Cottrel, B. M. Grossman, K. A. Salsburg, "Finite-element analysis of semiconductor devices-the FIELDAY program", IBM J. Res. Development, vol. 25, no. 4, pp 218-231, 1981.
- 22) G. D. Hachtel, M. H. Mack, R. R. O'Brien, B. Speelpenning, "Semiconductor analysis using finite elements", IBM J. Res. Development vol. 25, no. 4, pp 232-260, 1981.
- 23) R. S. Varga, "Matrix iterative analysis", Prentice-Hall Inc., Englewood Cliffs, N. J., 1962.
- 24) G. E. Forsythe, W. R. Wasow, "Finite-Difference Methods for Partial differential equations", John Wiley and sons Inc., N. Y., 1967

- 25) N. Gastinel, "Linear numerical analysis", Academic Press Inc., N.Y., 1970.
- 26) F. Hildebrand, "Finite Difference equations and simulations", Prentice-Hall Inc., Englewood Cliffs, N.J., 1968.
- 27) W.F. Ames, "Numerical methods for partial differential equations", Barnes and Noble Inc., N.Y., 1969.
- 28) D.M. Young, "Iterative solution of large linear systems", Academic Press Inc., N.Y., 1971.
- 29) H.L. Stone, "Iterative solution of implicit approximations of multidimensional partial differential equations", SIAM. J. Num. Anal., vol. 5, pp 530-558, 1968.
- 30) C. Canali, G. Majni, R. Minder, and G. Ottaviani, "Electron and hole drift velocity measurements in silicon and their empirical relation to electric field and temperature", IEEE Trans. Electron Devices, vol. ED-22, pp 1045-1047, 1975.
- 31) P.P. Debye and E.M. Conwell, "Electrical properties of n-type germanium", Phys. Rev., vol. 93, pp 693-706, 1954,
- 32) S. Selberherr, A. Schütz and H. Pötzl, "MINIMOS 2.0 User's guide, Technische Universität Wien, May 1982.
- 33) I. Gradshteyn, I.W. Ryzhik, "Table of integrals series and products", Academic Press Inc., N.Y., 1965.


```

DO 15 I=1,N-1
PHIP(I)=CJP*F(I)+PHIP(N)
15 PHIN(I)=CJN*FN(I)+PHIN(N)
DO 112 I=1,N
HC(I)=Z(I)*PHIP(I)
EC(I)=Y(I)*PHIN(I)
112 CONTINUE
C
IF(FINAL) CALL OUTPUT(5100)
C
C ***EVALUATE SECOND DERIVATIVE OF ELECTROSTATIC POTENTIAL***
C
M=N-2
DO 113 I=2,N-1
SDEP(I)=(EP(I+1)-2.*EP(I)+EP(I-1))/H**2
113 CONTINUE
C
C ***SOLUTION OF LINEARIZED POISSON,S EQUATION***
C
DO 311 I=1,N-2
A(I)=(EC(I+1)+HC(I+1))*H*H+2.
J(I)=(SDEP(I+1)-EC(I+1)+HC(I+1)+C(I+1))*H*H
311 CONTINUE
C
CALL FGETDS(M,A,D)
C
DO 81 I=2,N-1
EP(I)=EP(I)+D(I-1)
J=0
DO 3001 I=1,N-2
IF(ABS(D(I)).GT.EPS) GO TO 3001
J=J+1
3001 CONTINUE
IF(J.EQ.M) GO TO 1982
ITER=ITER+1
IF(ITER.LE.MAXIT) GO TO 55
C
C *** END OF ITERATION LOOP***
C
1982 CALL OUTPUT(5100)
FINAL=.TRUE.
GO TO 55
100 STOP
END
SUBROUTINE FGETDS(N,A,B)
C
C *** FAST GAUSSIAN ELIMINATION OF TRIANGONAL SYSTEMS***
C
DIMENSION A(N),B(N)
DO 10 I=2,N
A(I)=A(I)-1./A(I-1)
3(I)=B(I)+3(I-1)/A(I-1)
10 CONTINUE
B(N)=B(N)/A(N)
DO 20 I=N-1,1,-1
3(I)=(3(I)+B(I+1))/A(I)
20 CONTINUE
RETURN
END
SUBROUTINE GUESOL
C
C ***A PROGRAM WHICH CALCULATES PIECEWISE LINEAR GUESS SOLUTIONS***
C
COMMON/PARAM/TEMP,DPL,DNL,CNI,CNA,CND,N,V,H,THV,DL,Q,CRA
COMMON/VAR/EP(100),C(100),X(100)
REAL LEVEL
T=TEMP+273.
IL=DPL+DNL
E0ER=1.8*9.85E-14
Q=1.6E-19
CNI=3.88E15*(T**1.5)*DEXP(-7000./T)
DL=SQRT((E0ER*1.38E-23*T)/(Q**2*CNI))
THV=1.38E-23*T/Q
PHIO=THV*LOG(CNA*CND/CNI**2)
CNAN=CNA/CNI
CNDN=CND/CNI
EP0=V-THV*DLOG(DSQRT(CNAN**2/4.+1.)+CNAN/2.)
TN=CNA+CND
XPD=DSQRT(2.*E0ER*(PHIO-V)*CND/(Q*CNA*TN))
XND=DSQRT(2.*E0ER*(PHIO-V)*CNA/(Q*CND*TN))
JW=(XPD+XND)/DL
IF(V.GT.PHIO) V=PHIO

```



```

*=-15.8)
IF(OPT.EQ.,NN,) RETURN 1
IF(OPT.EQ.,NY,) GO TO 1
PRINT 5011
5011 FORMAT(1H1,5(/),3X,,ELECTROSTATIC POTENTIAL,,4X,,HOLE CONCENTRATIO
*V,,4X,,ELECTRON CONCENTRATION,,4X,,HOLE QUASI FERMI LEVEL,,4X,,ELE
*CTRON QUASI FERMI LEVEL,,//)

```

C

```

1 DO 31 I=1,N
EP(I)=EP(I)*THV
HC(I)=HC(I)*CNI
EC(I)=EC(I)*CNI
AB(I)=DLOG(PHIP(I))*THV
X(I)=X(I)*DL
C(I)=C(I)*CNI
CD(I)=-DLOG(PHIN(I))*THV
IF(OPT.EQ.,NY,) GO TO 31
PRINT 5012,I,EP(I),HC(I),EC(I),AB(I),CD(I)
5012 FORMAT(1X,I3,4X,F11.8,14X,E9.4,12X,E9.4,13X,F11.8,15X,F11.8)
31 CONTINUE
IF(OPT.EQ.,YN,) RETURN 1

```

C

```

CALL GRAPH4(10.5,9.,N,X,EP)
PRINT 5013
5013 FORMAT(/,50X,,ELECTROSTATIC POTENTIAL,)
CALL GRAPH4(10.5,9.,N,X,HC)
PRINT 5014
5014 FORMAT(/,50X,,HOLE CONCENTRATION,)
CALL GRAPH4(10.5,9.,N,X,EC)
PRINT 5015
5015 FORMAT(/,50X,,ELECTRON CONCENTRATION,)
CALL GRAPH4(10.5,9.,N,X,AB)
PRINT 5016
5016 FORMAT(/,50X,,HOLE QUASI FERMI LEVEL,)
CALL GRAPH4(10.5,9.,N,X,CD)
PRINT 5017
5017 FORMAT(/,50X,,ELECTRON QUASI FERMI LEVEL,)
CALL GRAPH4(10.5,9.,N,X,C)
PRINT 5018
5018 FORMAT(/,50X,,DOPING PROFILE,)
RETURN 1
END

```

PRINTS

ONE DIMENSIONAL STEADY STATE ANALYSIS OF SILICON DIODES

ACCEPTOR DENSITY (PER CUBIC CENTIMETERS) = $.10 \times 10^{17}$

DONOR DENSITY (PER CUBIC CENTIMETERS) = $.10 \times 10^{19}$

DIODE DIMENSIONS (CENTIMETERS)

P-SIDE = $.1000 \times 10^{-3}$ N-SIDE = $.1000 \times 10^{-3}$

CROSSSECTIONAL AREA (SQUARE CENTIMETERS) = $.00100000$

TEMPERATURE (DEGREES CELSIUS) = 25.00

BIAS VOLTAGE = .3000

FINAL RESULTS

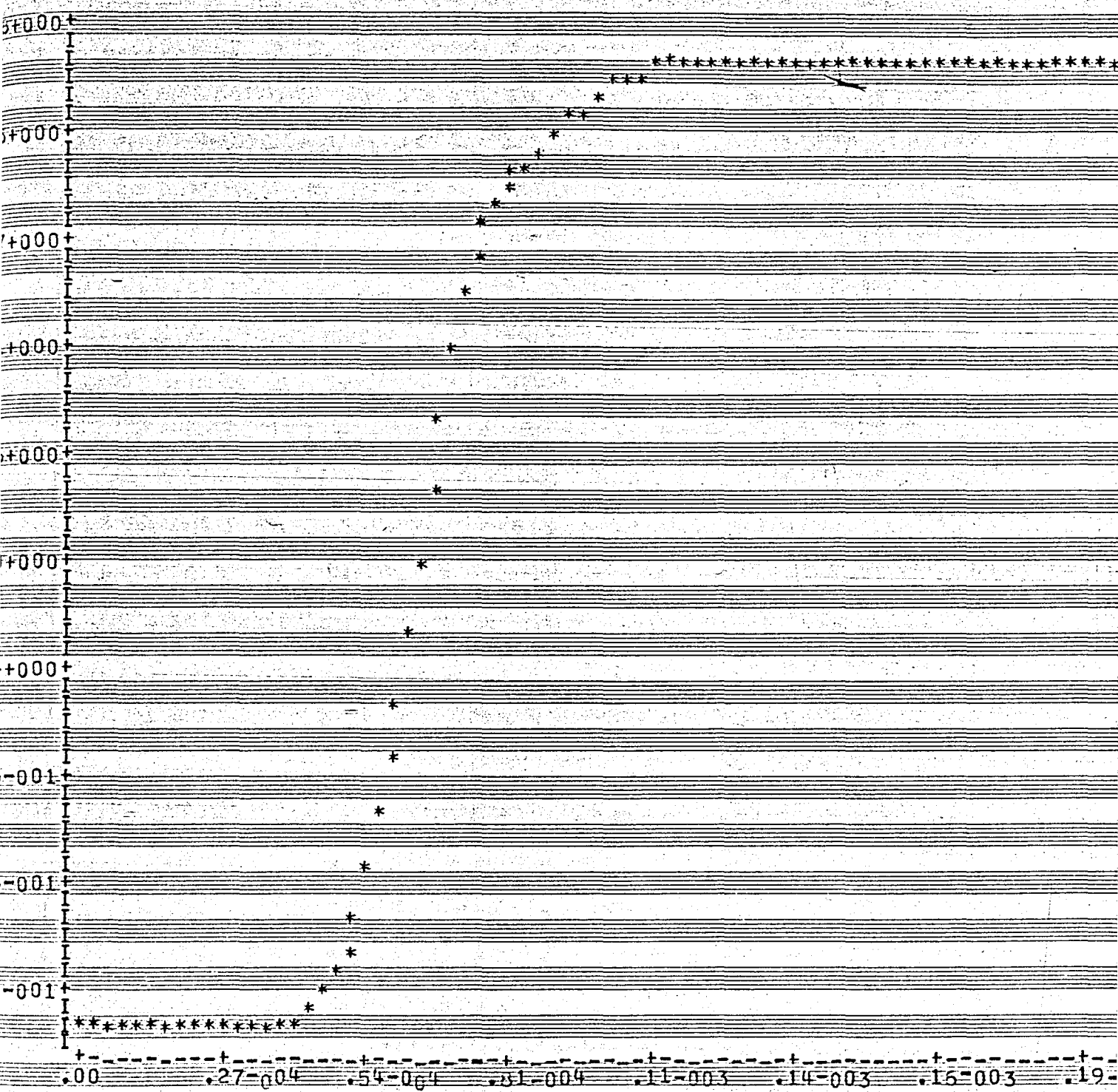
ITERATIONS DONE = 44

INTRINSIC CARRIER CONCENTRATION (PER CUBIC CENTIMETERS) = $.1255 \times 10^{11}$

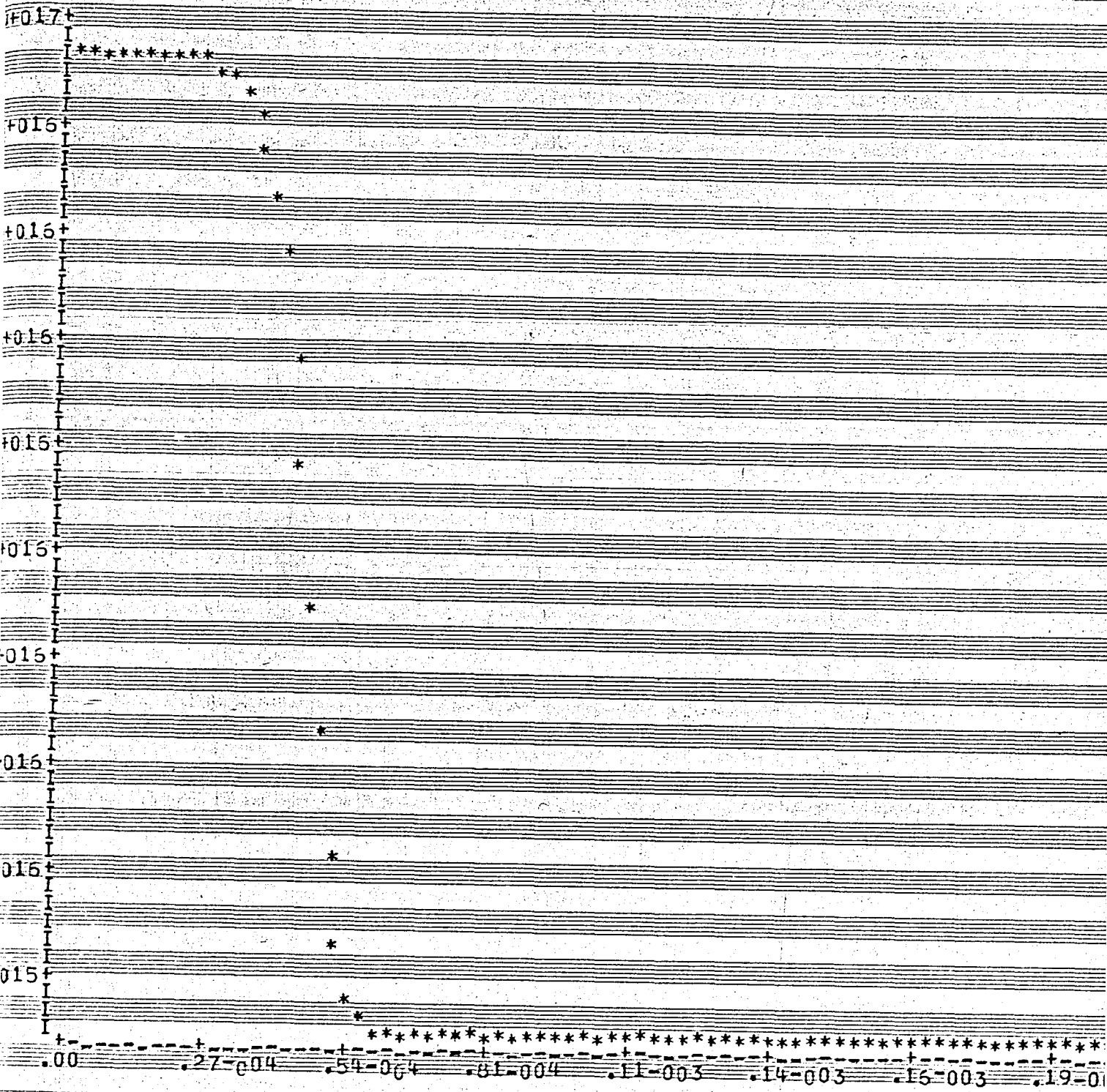
HOLE CURRENT DENSITY (AMPERES PER SQUARE CENTIMETERS) = $.36647708 \times 10^{-6}$

ELECTRON CURRENT DENSITY (AMPERES PER SQUARE CENTIMETERS) = $.22049851 \times 10^{-3}$

DIODE CURRENT (AMPERES) = $.22086503 \times 10^{-6}$



ELECTROSTATIC POTENTIAL



HOLE CONCENTRATION

.35+000

.31+000 *

.27+000

.23+000

.19+000

.14+000

.10+000

.62-001 *

.21-001

**

**

*

**

*

00

.27-004

.54-004

.61-004

.11-003

.14-003

.16-003

.19-003

.22-003

.24-003

ELECTRON QUASI FERMI LEVEL


```

1. *
2. IMPLICIT REAL*8 (A-H,O-Z)
3. DIMENSION D(200),SDEP(200),Y(200),Z(200),A(200)
4. COMMON /VAR/ EP(200),C(200),X(200),VEB,VCB,EAC,BDC,CAC
5. COMMON/PARAM/TEMP,WE,WB,WC,CNI,N,THV,DL,O,CRA,H
6. COMMON/PARAM1/CJP,CJNE,CJNC,F(200),FNE(200),FNC(200),ITER,M
7. COMMON/VAR1/HC(200),EC(200),PHIP(200),PHIN(200)
8. LOGICAL FINAL
9. *
10. *
11. READ(5,1)N
12. READ(5,2)WE,WB,WC,CRA
13. READ(5,3)TEMP,VEB,VCB
14. READ(5,4)EAC,BDC,CAC
15. *
16. *
17. 1 FORMAT(I3)
18. 2 FORMAT(4E10.4)
19. 3 FORMAT(3F5.2)
20. 4 FORMAT(3E10.4)
21. *
22. MID=94
23. MAXIT=200
24. EPS=0.00001
25. ITER=1
26. FINAL=.FALSE.
27. *
28. CALL OUTPUT(599,5100)
29. 99 CALL GUESOL
30. *
31. HQFPI=VEB/THV
32. HQFPN=VCB/THV
33. EQFPI=HQFPI
34. EQFPN=HQFPN
35. *
36. * ***ITERATION LOOP BEGINS***
37. *
38. 55 DO 104 I=1,N
39. Y(I)=DEXP(EP(I))
40. 104 Z(I)=DEXP(-EP(I))
41. *
42. FNE(I)=0.
43. FNC(I)=0.
44. F(N)=0.
45. *
46. DO 111 I=N,2,-1
47. 111 F(I-1)=(Y(I-1)+Y(I))*H/Z.+F(I)
48. DO 121 I=2,MID
49. 121 FNE(I)=(Z(I)+Z(I-1))*H/2.+FNE(I-1)
50. DO 122 I=2,N-MID+1
51. J=I+MID-1
52. 122 FNC(I)=(Z(J-1)+Z(J))*H/2.+FNC(I-1)
53. PHIP(N)=DEXP(HQFPN)
54. CJP=(DEXP(HQFPI)-PHIP(N))/F(I)
55. DO 15 I=1,N-1
56. 15 PHIP(I)=CJP*F(I)+PHIP(N)
57. CJNE=(1.-DEXP(-EQFPI))/FNE(MID)
58. CJNC=(EXP(-EQFPN)-1.)/FNC(N-MID+1)
59. PHIN(1)=DEXP(-EQFPI)
60. * PHIN(N)=DEXP(-EQFPN)
61. DO 16 I=2,N
62. IF(I.GT.MID) GO TO 17
63. PHIN(I)=CJNE*FNE(I)+PHIN(1)
64. GO TO 16
65. 17 PHIN(I)=CJNC*FNC(I-MID+1)+1.
66. 16 CONTINUE

```

```

70.      I12 CONTINUE
71.      *
72.      IF(FINAE) CALL OUTPUT($99,$100)
73.      *
74.      * ***SOLUTION OF LINEARIZED POISSON'S EQUATION***
75.      *
76.      M=N-2
77.      DO 113 I=2,N-1
78.      SDEP(I)=(EP(I+1)-2.*EP(I)+EP(I-1))/H**2
79.      I13 CONTINUE
80.      *
81.      DO 311 I=1,M
82.      A(I)=(EC(I+1)+HC(I+1))*H*H+2.
83.      D(I)=(SDEP(I+1)-EC(I+1)+HC(I+1)+C(I+1))*H*H
84.      311 CONTINUE
85.      *
86.      CALL FGETDS(M,A,D)
87.      *
88.      DO 81 I=2,N-1
89.      81 EP(I)=EP(I)+D(I-1)
90.      *
91.      J=0
92.      DO 3001 I=1,M
93.      IF(ABS(DEF)) .GT. EPSIG0 GO TO 3001
94.      J=J+1
95.      3001 CONTINUE
96.      IF(J.EQ.M) GO TO 1982
97.      ITER=ITER+1
98.      IF(ITER.GE.MAXIT) GO TO 55
99.      *
100.     * *** END OF ITERATION LOOP***
101.     *
102.     CALL OUTPUT($99,$100)
103.     1982 FINAE=.TRUE.
104.     GO TO 55
105.     100 STOP
106.     END

```

```

107.     SUBROUTINE FGETDS(N,A,B)
108.     *
109.     * ***FAST GAUSSIAN ELIMINATION OF TRIDIAGONAL SYSTEMS***
110.     *
111.     IMPLICIT REAL*8 (A-H,O-Z)
112.     DIMENSION A(N),B(N)
113.     DO 10 I=2,N
114.     A(I)=A(I)-I./A(I-1)
115.     B(I)=B(I)+B(I-1)/A(I-1)
116.     10 CONTINUE
117.     B(N)=B(N)/A(N)
118.     DO 20 I=N-1,I,-1
119.     B(I)=(B(I)+B(I+1))/A(I)
120.     20 CONTINUE
121.     RETURN
122.     END

```

```

123.     SUBROUTINE GUESOL
124.     *
125.     IMPLICIT REAL*8 (A-H,O-Z)
126.     COMMON/VAR/ EP(200),C(200),X(200),VEB,VCB,EAC,BDC,CAC
127.     COMMON/PARAM/TEMP,WE,WB,WC,CNI,N,THV,DL,Q,CRA,H
128.     T=TEMP+273.
129.     CJ=WE+WB
130.     EDER=11.8*8.85E-14
131.     Q=1.6E-19

```

```

132.     CNI=3.88E16*(T**1.5)*DEXP(-7000./T)
133.     DL=SQRT((F0FR*T.38E-23*T)/(O**2*CNI))

```

```

137. EACN=EAC/CNI
138. BDCN=BDC/CNI
139. CACN=CAC/CNI
140. EPO=VEB/THV-DLOG(DSQRT(EACN**2/4.+1.)+EACN/2.)
141. EPN=VCB/THV-DLOG(DSQRT(CACN**2/4.+1.)+CACN/2.)
142. TN1=EAC+BDC
143. TN2=CAC+BDC
144. XPO1=DSQRT(2.*EQER*(PHI01-VEB)*BDC/(Q*EAC*TN1))
145. XPO2=DSQRT(2.*EQER*(PHI02-VCB)*BDC/(Q*CAC*TN2))
146. XNO1=DSQRT(2.*EQER*(PHI01-VEB)*EAC/(Q*BDC*TN1))
147. XNO2=DSQRT(2.*EQER*(PHI02-VCB)*CAC/(Q*BDC*TN2))
148. DW1=(XPO1+XNO1)/DL
149. DW2=(XPO2+XNO2)/DL
150. SLOPE1=(PHI01-VEB)/(DW1*THV)
151. SLOPE2=(PHI02-VCB)/(DW2*THV)

```

```

152. *
153. *   ***DEFINITION OF MESH***
154. *

```

```

155. H=(WE+WB+WC)/(DL*(N-1))
156. X(I)=0.
157. DO 102 I=2,N
158. X(I)=X(I-1)+H
159. 102 CONTINUE

```

```

160. *
161. *

```

```

162. *
163. P1=(WE-XPO1)/DL
164. P2=(WE+XNO1)/DL
165. P3=(CJ-XNO2)/DL
166. P4=(CJ+XPO2)/DL
167. DO 5 I=1,N
168. IF(X(I).GE.P1) GO TO 15
169. EP(I)=EPO
170. GO TO 5
171. 15 IF(X(I).GE.P2) GO TO 16
172. EP(I)=EP(I-1)+SLOPE1*H2
173. GO TO 5
174. 16 IF(X(I).GE.P3) GO TO 17
175. EP(I)=EPO+(PHI01-VEB)/THV
176. GO TO 5
177. 17 IF(X(I).GE.P4) GO TO 18
178. EP(I)=EP(I-1)-SLOPE2*H2
179. GO TO 5
180. 18 EP(I)=EPN
181. 5 CONTINUE

```

```

182. *
183. *   ***DEFINITION OF DOPING PROFILE***
184. *

```

```

185. P=600.
186. C(I)=-EACN
187. C(N)=-CACN
188. XO1=WE/DL
189. XO2=CJ/DL
190. DX=XO1+WB/(DL*2.)
191. DO 103 I=2,N-1
192. IF(X(I).GT.DX) GO TO 50
193. C(I)=-EACN+(EACN+BDCN)/(1.+EXP(-P*(X(I)-XO1)))
194. GO TO 103
195. 50 C(I)=-CACN+(CACN+BDCN)/(1.+EXP(P*(X(I)-XO2)))
196. 103 CONTINUE
197. RETURN
198. END

```

```

199. SUBROUTINE OUTPUT(*,*)
200. IMPLICIT REAL*8 (A-H,O-Z)
201. COMMON/VAR/EP(200),C(200),X(200),VEB,VCB,EAC,BDC,CAC
202. COMMON/PARAM/TEMP,WE,WB,WC,CNI,N,THV,DL,Q,CRA,H
203. COMMON/PARAM1/CJP,CJNE,CJNC,F(200),FNE(200),FNC(200),ITER
204. COMMON/VARI/HC(200),EC(200),PHIP(200),PHIN(200)
205. *
206. IF(ITER.NE.1) GO TO 9

```

```

212. PRINT 5003,BDC,CAC
213. 5003 FORMAT(10X,'BASE DGNOR DENSITY=',E9.2,5(/),10X,'COLLECTOR
214. *DENSITY=',E9.2,5(/))
215. PRINT 5004
216. 5004 FORMAT(10X,'DIMENSIONS OF TRANSISTOR',S(/))
217.
218. PRINT 5005,WE,WB,WC
219. 5005 FORMAT(10X,'EMITTER;',E10.4,5X,'BASE;',E10.4,5X,'COLLECTOR
220. *,5(/))
221. PRINT 5006,CRA
222. 5006 FORMAT(10X,'CROSSSECTIONAL AREA=',F10.9,5(/))
223. PRINT 5007,TEMP,VEB,VCB
224. 5007 FORMAT(10X,'TEMPERATURE=',F6.2,5(/),10X,'BIAS VOLTAGES',/10
225. *,5(/),10X,'VEB=',F6.2,10X,'VCB=',F6.2/10X,76('='))
226. PRINT 6001
227. 6001 FORMAT(5(/),10X,'*ALL DENSITIES ARE PER CUBIC CENTIMETERS,
228. *NS IN CENTIMETERS,AND TEMPERATURE IN DEGREES CELSIUS*')
229. RETURN 1
230. 9 IF(ITER.LE.MAXIT) GO TO 10
231. PRINT 5008
232. 5008 FORMAT(5(/),10X,'**MAXIMUM ITERATION LIMIT EXCEEDED EXECUT
233. *INATED***')
234. RETURN 2
235. 10 PRINT 5009,ITER
236. 5009 FORMAT(5(/),10X,'FINAL RESULTS',/10X,13('='),4(/),10X,'IT
237. * DONE=',I3)
238. UCD=Q*CNI/DL
239. HCD=CJP*480.*THV*UCD
240. ECDC=CJNC*1350.*THV*UCD
241. ECR=(HCD+ECDE)*CRA
242. CCR=(HCD+ECDC)*CRA
243. BCR=(ECDE-ECDC)*CRA
244. PRINT 5010,CNI
245. 5010 FORMAT(5(/),10X,'INTRINSIC CARRIER CONCENTRATION=',E12.4,5
246. PRINT 6002,ECR,BCR,CCR
247. 6002 FORMAT(10X,'STEADY STATE TERMINAL CURRENTS(AMP)',/10X,30('
248. *5(/),10X,'EMITTER:',E15.8,5X,'BASE:',E15.8,5X,'COLLECTOR:'
249. *
250. *
251. *
252. CALL GRALIS(EP,HC,EC,PHIP,PHIN,X,C,N,THV,DL,CNI)
253. RETURN 2
254. END

```

```

255. SUBROUTINE GRALIS(EP,HC,EC,PHIP,PHIN,X,C,N,THV,DL,CNI)
256. DIMENSION SEP(200),SHC(200),SEC(200),AB(200),CD(200)
257. * ,SX(200),SC(200)
258. REAL*8 THV,CNI,DL
259. DOUBLE PRECISION EP(N),HC(N),EC(N),PHIP(N),PHIN(N),X(N),C(N)
260. PRINT 5011
261. 5011 FORMAT(1H1,5(/),3X,'ELECTROSTATIC POTENTIAL',4X,'HOLE CONC
262. *N',4X,'ELECTRON CONCENTRATION',4X,'HOLE QUASI FERMI LEVEL'
263. *CTRON QUASI FERMI LEVEL',///)
264. DO 31 I=1,N
265. SEP(I)=EP(I)*THV
266. SHC(I)=HC(I)*CNI
267. SEC(I)=EC(I)*CNI
268. AB(I)=DLOG(PHIP(I))*THV
269. CD(I)=-DLOG(PHIN(I))*THV
270. SX(I)=X(I)*DL
271. SC(I)=C(I)*CNI
272. PRINT 5012,I,SEP(I),SHC(I),SEC(I),AB(I),CD(I)
273. 5012 FORMAT(1X,13,4X,F11.8,16X,E9.4,15X,E9.4,16X,F11.8,17X,F11.
274. 31 CONTINUE
275. CALL GRAPH4(10.5,9.,N,SX,SEP)
276. PRINT 5013
277. 5013 FORMAT(///,50X,'ELECTROSTATIC POTENTIAL')
278. CALL GRAPH4(10.5,9.,N,SX,SHC)
279. PRINT 5014
280. 5014 FORMAT(///,50X,'HOLE CONCENTRATION')
281. CALL GRAPH4(10.5,9.,N,SX,SEC)

```

```

282. PRINT 5015
283. 5015 FORMAT(///,50X,'ELECTRON CONCENTRATION')

```

```
285. PRINT 5016
286. 5016 FORMAT(///,50X,'HOLE QUASI-FERMI LEVEL')
287. CALL GRAPH4(10.5,9.,N,SX,CD)
288. PRINT 5017
289. 5017 FORMAT(///,50X,'ELECTRON QUASI-FERMI LEVEL')
290. CALL GRAPH4(10.5,9.,N,SX,SC)
291. PRINT 5018
292. 5018 FORMAT(///,50X,'DOPING PROFILE')
293. RETURN
294. END
```

ONE DIMENSIONAL STEADY STATE ANALYSIS OF SILICON BIPOLEAR TRANSISTOR

EMITTER ACCEPTOR DENSITY= $.10 \times 10^{18}$

BASE DONOR DENSITY= $.10 \times 10^{17}$

COLLECTOR ACCEPTOR DENSITY= $.10 \times 10^{18}$

DIMENSIONS OF TRANSISTOR

EMITTER; $.1000 - 003$ BASE; $.1000 - 003$ COLLECTOR; $.1000 - 003$

CROSS SECTIONAL AREA= $.000100000$

TEMPERATURE= 25.00

BIAS VOLTAGES

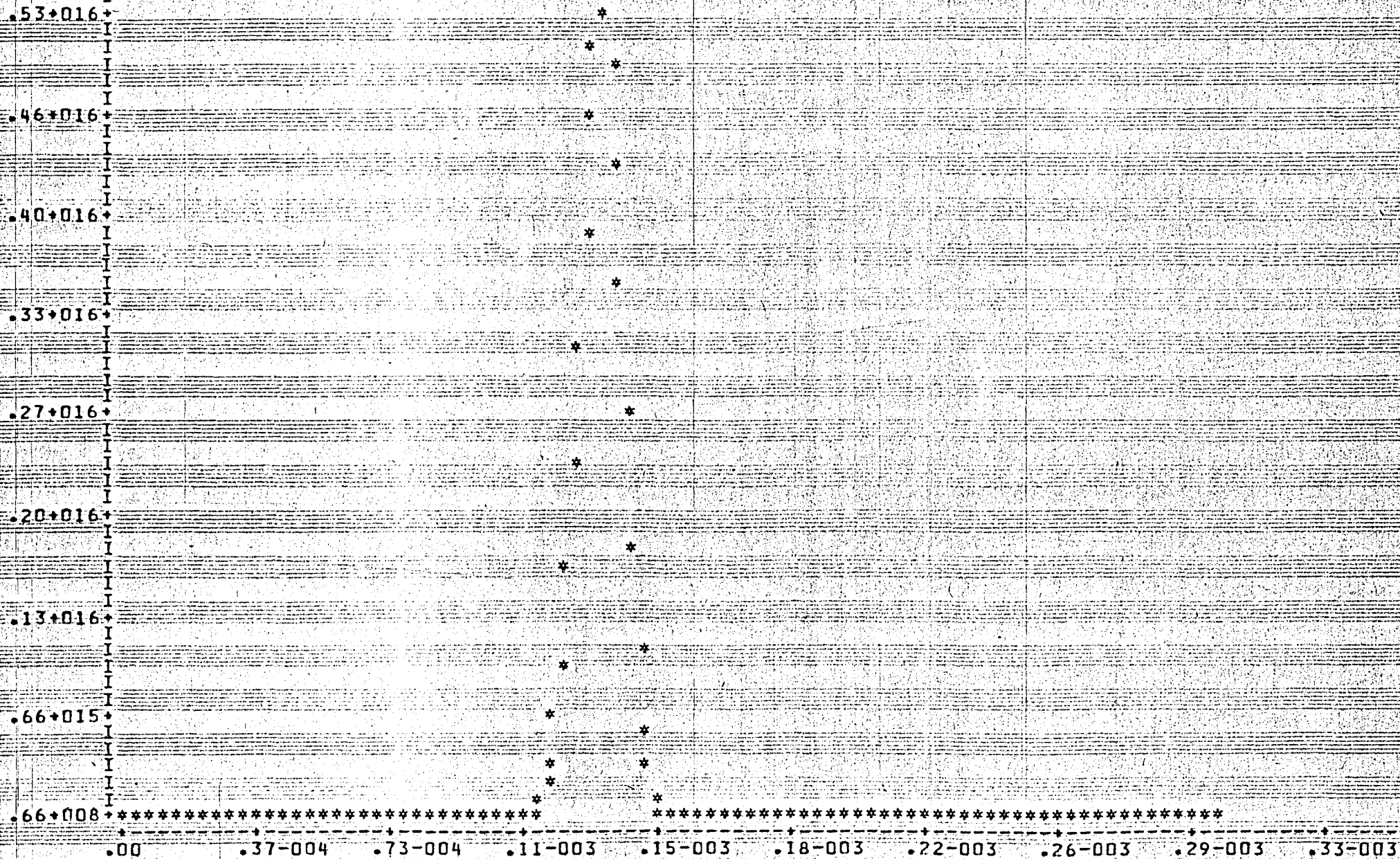
$V_{EB} = .50$ $V_{CB} = -2.00$

*ALL DENSITIES ARE PER CUBIC CENTIMETERS, DIMENSIONS IN CENTIMETERS, AND TEMPERATURE IN DEGREES CELSIUS

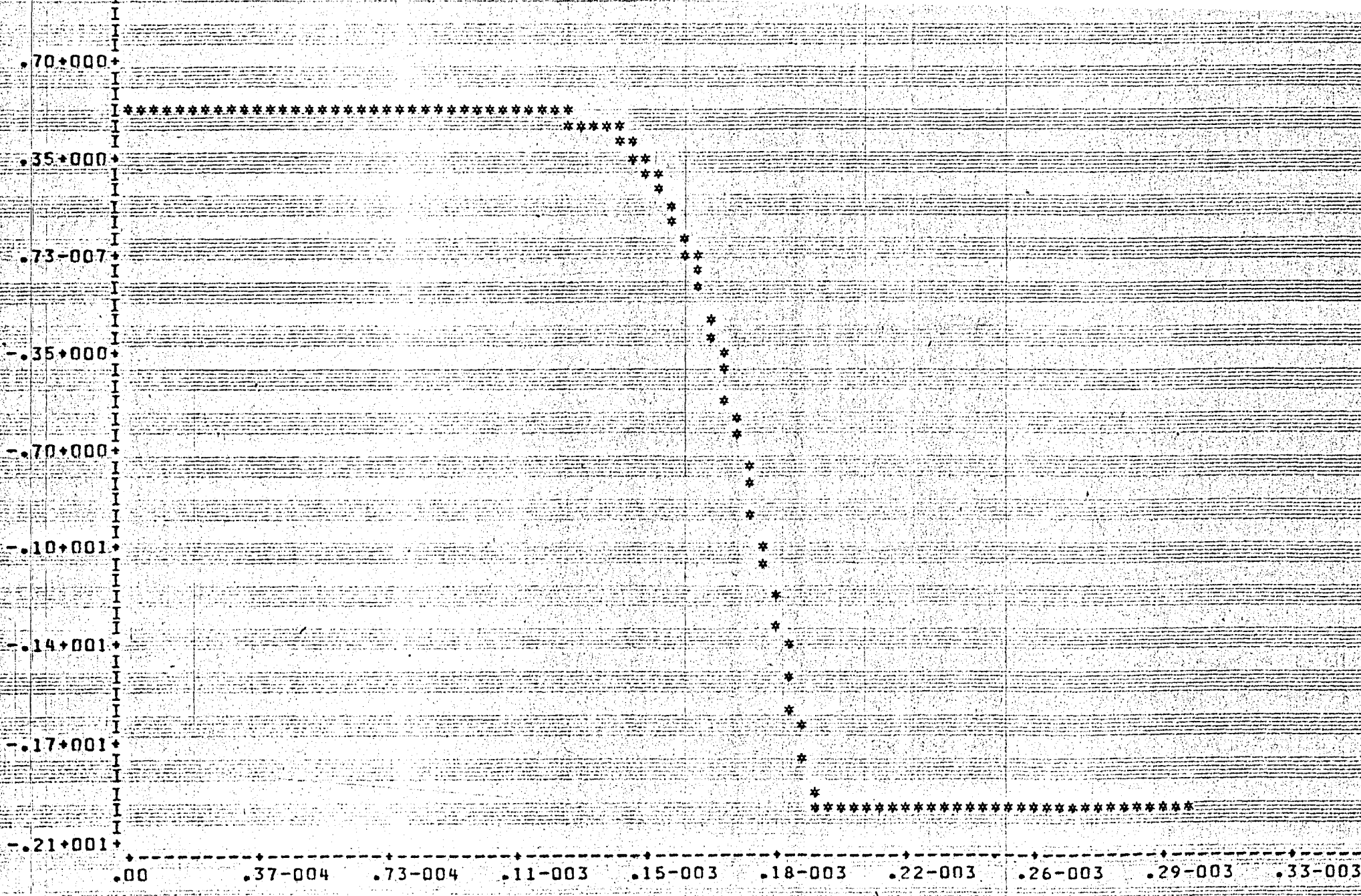
FINAL RESULTS

ITERATIONS DONE= 10

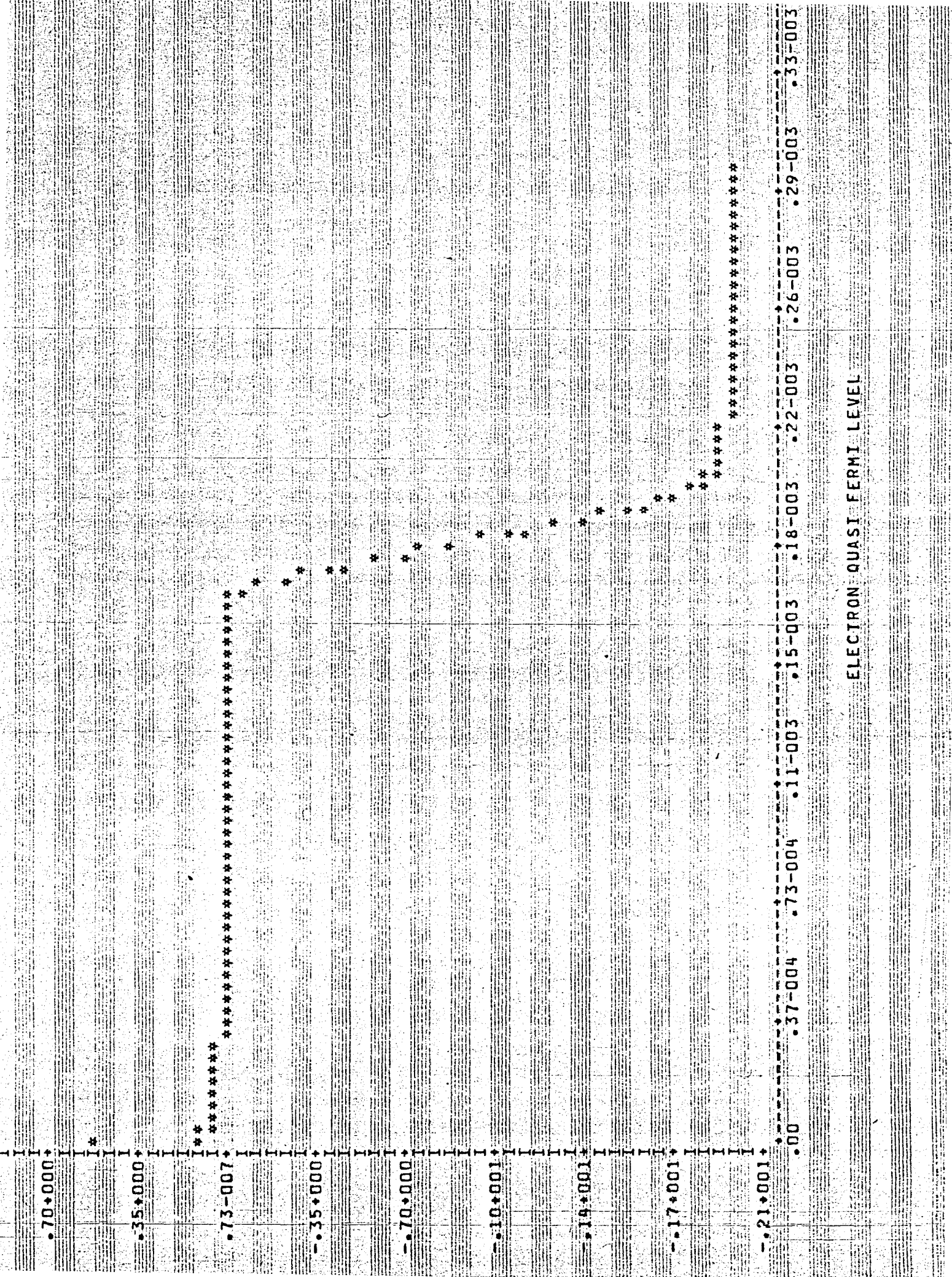
INTRINSIC CARRIER CONCENTRATION= $.1255 \times 10^{11}$



ELECTRON CONCENTRATION



HOLE QUASI FERMI LEVEL



ELECTRON QUASI FERMI LEVEL

